The 2010 stock assessment of paua (*Haliotis iris*) for Milford, George, Central, and Dusky in PAU 5A

D. Fu
A. McKenzie

NIWA
Private Bag 14901
Wellington 6241

New Zealand Fisheries Assessment Report 2010/46
December 2010

Published by Ministry of Fisheries
Wellington
2010

ISSN 1175-1584 (print)
ISSN 1179-5352 (online)

Fu, D.; McKenzie, A. (2010).
The 2010 stock assessment of paua (*Haliotis iris*) for Milford, George, Central, and Dusky in PAU 5A.
New Zealand Fisheries Assessment Report 2010/46.

This series continues the informal
New Zealand Fisheries Assessment Research Document series
which ceased at the end of 1999.

EXECUTIVE SUMMARY

Fu, D.; McKenzie, A. (2010). The 2010 stock assessment of paua (*Haliotis iris*) for Milford, George, Central, and Dusky in PAU 5A.

New Zealand Fisheries Assessment Report 2010/46.

The stock assessments for PAU 5A have previously been carried out at the QMA level. In 2010 the Shellfish Working Group decided to conduct the stock assessment for the two subareas of PAU 5A separately: a southern area including Chalky and South Coast, and a northern area including Milford, George, Central, and Dusky. The decision was made to address the differences in exploitation histories between subareas within PAU 5A, and to reflect recent changes in management measures within the fishery.

This report summarises the stock assessment for the northern area of PAU 5A and includes fishery data from Milford, George, Central, and Dusky until the 2009–10 fishing year. The report describes the model structure and output, including current and projected stock status. The stock assessment is implemented as a length-based Bayesian estimation model, with point estimates of parameters based on the mode of the joint posterior distribution. The uncertainty of model estimates is investigated using the marginal posterior distributions generated from Markov chain-Monte Carlo simulation.

The model dynamics used for this assessment are the same as those used in the southern area assessment, and are also similar to those of previous assessments of PAU 5A, but with minor modifications to accommodate the changes in the minimum harvest size. The data fitted in the assessment model were: (1) a standardised CPUE series based on the early CELR data, (2) a standardised CPUE series covering based on recent PCELR data, (3) a standardised research diver survey index (RDSI), (4) a research diver survey proportions-at-length series, (5) a commercial catch sampling length frequency series, (6) tag-recapture length increment data, and (7) maturity-at-length data.

The catch history used as the model input included commercial, recreational, customary, and illegal catch. The commercial catch history estimates between 1984 and 2010 were based on reported catch from Statistical Areas 031 and 032, and estimates before 1984 were made using assumptions about the split of the catch between subareas within PAU 5A. The split proportions were inferred from the total estimated catch between 1984 and 95 from Statistical Areas 030, 031, and 032, assuming that 18% (upper bound), 40% (base case), or 61% (lower bound) of the annual catch in 030 was taken from PAU 5A.

The maturity and growth data included in the model were based on samples collected throughout PAU 5A, and the abundance and length frequency data were from Milford, George, Central, and Dusky. As for the southern area assessment, only four years of catch sampling length frequencies (2002–05) were included, as the sampling coverage has been low since then and is unreliable before 2002. The decision was made following the southern area assessment.

Iterative re-weighting of the datasets produced an initial model run in which the standard deviations of the normalised residuals were close to unity for each dataset. Most datasets were fitted well except that the fitted CPUE between 2002 and 2009 showed a steeper decline than the observed CPUE. A base case run was proposed which up-weighted the recent CPUE and resulted in improved fits. The base case suggested that the spawning stock population in 2010 (B_{current}) is 41% (34%–50%) B_0, and the recruit-sized stock abundance ($B^r_{current}$) is 26% (21%–33%) of initial state (B^r_0). An alternative model was also implemented which assumed a non-linear relationship between CPUE and vulnerable biomass (hyperstability model). This model suggested that B_{current} is 26% (21%–35%) B_0, and recruit-sized stock abundance ($B^r_{current}$) is 16% (12%–22%) of initial state (B^r_0).

The model projections made for 2 years assuming current catch levels, and using recruitments re-sampled from the recent model estimates, suggested that the stock abundance will decrease slightly over the next two years. The spawning stock biomass in 2012 is projected to be 40% (32–50%) B_0 for the base case, and 25% (19–33%) for the hyperstability model. The projections suggested that the probability of the biomass increasing in two years time will be greater than 50% if the future catch is reduced by 10 t for the base case model and by 20 t for the hyperstability model.

The model presented here, whilst fairly representing most of the data, also shows some indications of lack of fit. It is unlikely the estimates of historical stock size are reliable, given assumptions about annual recruitment and the use of the historical catch-effort as an index of abundance. The inter-annual variability of the research diver survey indices can not be explained by the model. Sensitivity runs indicated that the model is generally insensitive to the omission of a particular dataset except for the research diver length frequency data.

Another source of uncertainty in this model relates to changes in fishing selectivity due to an increase in minimum harvest size in 2007, which varied by region. The base case and hyperstability model assumed a shift of fishing selectivity by 2 mm since 2007, with alternatives of 3 and 4 mm investigated in sensitivity trials. When the assumed selectivity change ranged from 2 mm to 4 mm, the median B_{current} ranged from 41% to 50% for the base case, and from 26 to 30% of B_0 for the hyperstability model. The change in fishing selectivity since 2007 could not be quantified from the recent commercial catch length frequecey data, as the sampling coverage of the commercial catch was poor and changed over time.

1. INTRODUCTION

1.1 Overview

PAU 5A was last assessed in 2006 (Breen & Kim 2007) and before that in 2004 (Breen & Kim 2004b). The previous stock assessments for PAU 5A have been conducted assuming a homogenous stock throughout the whole PAU 5A.

There have been concerns regarding the applicability of previous assessments of the entire QMA, although there was general agreement that biomass decline had occurred in the southern region of the QMA over recent years. Recent studies suggested that trends in the changes of abundance may have varied between subareas within PAU 5A (Cordue 2009). Therefore a model assuming a homogenous area is unlikely to reflect the different exploitation histories between subareas, or to reliably predict the current status of the stock.

Since 1 October 2006, a voluntary subdivision was agreed to which divided PAU 5A into six fishing management zones, based on the research strata (Figure 1), and a proportion of the total annual catch entitlements (ACE) was allocated to each zone. Each of the management zones has a voluntary harvest cap and minimum harvest length in place.

The Shellfish Working Group (SFWG) suggested conducting the 2010 assessment for two subareas of PAU 5A separately: the southern strata including Chalky and South Coast, and the northern strata including Milford, George, Central, and Dusky. The choice was tentatively based on availability of data, differences in exploitation history, and differences in management initiatives.

This report summarises the stock assessment for the northern strata of PAU 5A (Milford, George, Central, and Dusky) with the inclusion of fishery data until the 2009–10 fishing year. The stock assessment is made with the length-based Bayesian estimation model first used in 1999 for PAU 5B (Breen et al. 2000a) and revised for subsequent assessments in PAU 5B (Breen et al. 2000b) and PAU 7 (Andrew et al. 2000, Breen & Kim 2003, 2005, McKenzie & Smith 2009) with revisions made for PAU 4 (Breen & Kim 2004a) and PAU 5A (Breen & Kim 2004b) in 2004 mostly discarded. The model was published by Breen et al. (2003). The assessment for the southern area was reported in a separate document (Fu & McKenzie 2010).

The seven sets of data fitted in the assessment model were: (1) a standardised CPUE series covering 1990–2001 based on CELR data (CPUE), (2) a standardised CPUE series covering 2002–2009 based on PCELR data (PCPUE), (3) a standardised research diver survey index (RDSI), (4) a research diver survey proportions-at-lengths series (RDLF), (5) a commercial catch sampling length frequency series (CSLF), (6) tag-recapture length increment data, and (7) maturity-at-length data. Catch history was also an input to the model, encompassing commercial, recreational, customary, and illegal catch. A separate document describes the datasets that are used in the stock assessment and updates that were made for the previous assessment (Fu et al. 2010).

The assessment was made in several steps. First, the model was fitted to the data with arbitrary weights on the various data sets. The weights were then iteratively adjusted to produce balanced residuals among the datasets where the standardised deviation of the normalised residuals was close to one for each dataset. The fit obtained is the mode of the joint posterior distribution of parameters (MPD). Next, from the resulting fit, Markov chain-Monte Carlo (MCMC) simulations were made to obtain a large set of samples from the joint posterior distribution. From this set of samples, forward projections were made with a set of agreed indicators obtained. A number of model runs were explored by comparing MPD fits with the aim to find a base case run that best represents the data.

This document describes the model, the assumptions made in fitting, the fit of the model to the data, projection results, and sensitivity trials. This report fulfils Objective 1 “To update the stock assessment for PAU 5A, including estimates of abundance from the fisheries independent dive surveys from Objective 1, in February/March 2010" of Project PAU2007/03.

1.2 Description of the fishery

PAU 5A includes the coastal areas and islands of Fiordland (Figure 1), from the Waiau River (west of Riverton) to Awarua Point (north of Big Bay), The TACC for PAU 5A has remained at the initial level of 145 t since the 1995–96 fishing year. Landings have been close to the TACC since 1998–99 (Ministry of Fisheries 2009).

The paua fishery was summarised by Schiel (1992), and in numerous previous assessment documents (e.g., Schiel 1989, McShane et al. 1994, 1996, Breen et al. 2000a, 2000b, 2001, Breen & Kim 2003, 2004a, 2004b, 2007), and more recently by Fu (unpublished). A brief summary of the recent changes in management measures is given below.

Since 1 October 2006, a voluntary catch reduction of 30% has been in place and each of the management zones has a voluntary harvest cap. The only exception is in the Milford area where there is no limit on the catch. The harvest caps are designed to spread harvesting across the fishery and in particular to reduce effort in the southern three zones (Dusky, Chalky, and South Coast). This effectively reduces the allowable catch from 148 983 kg to 104 290 kg and has reduced the catch in the southern three zones by 50%. Initially the shelving was for 3 years but at the 2009 PauaMac5 AGM it was agreed to roll this over for another 2 years, reviewable annually.

An increased minimum harvest size (MHS) on top of the current Minimum Legal Size (MLS) in place was also implemented in some parts of the fishery from 1 October 2006, where the MHS was increased to 127 mm in southern Milford and George, and to 130 mm in Central and Dusky. There was no change in the MHS in the northern part of Milford.

2. MODEL

This section gives an overview of the model used for stock assessment of Milford, George, Central, and Dusky in 2010; for full details see Breen et al. (2003). The model was developed for use in PAU 5B in 1999 and has been revised each year for subsequent assessments, in many cases echoing changes made to the rock lobster assessment model Kim et al. 2004), which is a similar but more complex length-based Bayesian model. Only minor changes were made to the last revision which was the 2008 assessment model of PAU 7 (McKenzie & Smith 2009). The model is the same as that used for the stock assessment of Chalky and South Coast in 2010 (Fu & McKenzie 2010).

2.1 Changes to the 2008 assessment model of PAU 7

Only one minor change was made, allowing the selectivity to be shifted, due to a voluntary increase of MHS change from October 2007:

$$V_k^{t,s} = \frac{1}{1+19^{-\left(\left(l_k - D_{50} - E_t\right)/D_{95-50}\right)}}$$

where $E_t = 0$ for $t < 2007$ or $E_t = 2$ for $t \geq 2007$

The MHS increased to 127 mm in southern Milford and George, 130 mm in Central and Dusky, and remained unchanged in northern Milford. As the model was based on one fishery area, we assumed the selectivity was shifted by 2 mm ($E_t = 2$) since 2007 for the base case. Alternatively, a shift of 3 or 4 mm was explored in sensitivity trials (see Section 2.2.12).

2.2 Model description

The model partitioned paua stock into a single sex population, with length classes from 70 to 170 mm, in groups of 2 mm (i.e., from 70 to under 72 mm, 72 mm to under 74 mm, etc.). The largest length bin is well above the maximum size observed. The stock was assumed to reside in a single, homogeneous area. The partition accounted for numbers of paua by length class within an annual cycle, where movement between length classes was determined by the growth parameters. Paua entered the partition following recruitment and were removed by natural mortality and fishing mortality.

The model's annual cycle was based on the fishing year. Note that model references to "year" within this paper refer to the fishing year, and are labelled as the most recent calendar year, i.e., the fishing year 1998–99 is referred to as "1999" throughout. References to calendar years are denoted specifically.

The model was run for the years 1965–2010. Catches were available for 1974–2010 (catch in 2010 was assumed to be the harvest cap), and were assumed to increase linearly between 1965 and 1973 from 0 to the 1974 catch level. Catches included commercial, recreational, customary, and illegal catch, and all catches occurred at the same time step.

Recruitment was assumed to take place at the beginning of the annual cycle, and length at recruitment was defined by a uniform distribution with a range between 70 and 80 mm. Recruitment deviation was assumed known and equal to 1 for the years up to 1982 — 10 years before the first available length data were available (loosely based on the approximate time taken for recruited paua to appear at the right hand end of the length distribution). The stock-recruitment relationship is unknown for paua, but is likely to be weak or equivocal (Shepherd et al. 2001). A relationship may exist on small scales, but not be apparent when large-scale data are modelled (Breen et al. 2003). No explicit stock-recruitment relationship was modelled in this assessment.

Maturity does not feature in the population partition. The model estimated proportions mature with the inclusion of length-at-maturity data. Growth and natural mortalities were also estimated within the model.

The model used two selectivities: the commercial fishing selectivity and research diver survey selectivity — both assumed to follow a logistic curve (see later). The survey selectivity remained constant, and the commercial fishing selectivity was shifted by 2 mm for 2007–12 (assuming changes in definition of minimum harvest size extend to the projection period).

The model is implemented in AD Model Builder™ (Otter Research Ltd., http://otter-rsch.com/admodel.htm) version 9.0.65, compiled with the MinGW 3.45 compiler.

2.2.1 Estimated parameters

Parameters estimated by the model are as follows. The parameter vector is referred to as θ.

$\ln(R0)$	natural logarithm of base recruitment
M	instantaneous rate of natural mortality
g_α	expected annual growth increment at length α
g_β	expected annual growth increment at length β
ϕ	c.v. of the expected growth increment
q^I	scalar between recruited biomass and CPUE
X	coefficient of proportionality between q^I and q^{I2}, the scalar for PCPUE
q^J	scalar between numbers and the RDSI
L_{50}	length at which maturity is 50%
L_{95-50}	interval between L_{50} and L_{95}
T_{50}	length at which research diver selectivity is 50%
T_{95-50}	distance between T_{50} and T_{95}
D_{50}	length at which commercial diver selectivity is 50%
D_{95-50}	distance between D_{50} and D_{95}
$\tilde{\sigma}$	common component of error
h	shape of CPUE *vs.* biomass relation
ε	vector of annual recruitment deviations, estimated from 1977 to 2004

2.2.2 Constants

l_k	length of a paua at the midpoint of the k^{th} length class (l_k for class 1 is 71 mm, for class 2 is 73 mm and so on)
σ_{MIN}	minimum standard deviation of the expected growth increment (assumed to be 1 mm)
σ_{obs}	standard deviation of the observation error around the growth increment (assumed to be 0.25 mm)
MLS_t	minimum legal size in year *t* (assumed to be 125 mm for all years)
$P_{k,t}$	a switch based whether abalone in the k^{th} length class in year *t* are above the minimum legal size (MLS) ($P_{k,t} = 1$) or below ($P_{k,t} = 0$)
a, b	constants for the length-weight relation, taken from Schiel & Breen (1991) (2.592E-08 and 3.322 respectively, giving weight in kg)
w_k	the weight of an abalone at length l_k
ϖ^I	relative weight assigned to the CPUE dataset. This and the following relative weights were varied between runs to find a basecase with balanced residuals
ϖ^{I2}	relative weight assigned to the PCPUE dataset
ϖ^J	relative weight assigned to the RDSI dataset
ϖ^r	relative weight assigned to RDLF dataset
ϖ^s	relative weight assigned to CSLF dataset

ϖ^{mat} relative weight assigned to maturity-at-length data

ϖ^{tag} relative weight assigned to tag-recapture data

κ_t^s normalised square root of the number measured greater than 113 mm in CSLF records for each year, normalised by the lowest year

κ_t^r normalised square root of the number measured greater than 89 mm in RDLF records for each year, normalised by the lowest year

$U^{\max}$ exploitation rate above which a limiting function was invoked (0.80 for the base case)

μ_M mean of the prior distribution for *M*, based on a literature review by Shepherd & Breen (1992)

σ_M assumed standard deviation of the prior distribution for *M*

σ_ε assumed standard deviation of recruitment deviations in log space (part of the prior for recruitment deviations)

n_ε number of recruitment deviations

α length associated with g_α (75 mm)

β length associated with g_β (120 mm)

2.2.3 Observations

C_t observed catch in year *t*

I_t standardised CPUE in year *t*

$I2_t$ standardised PCPUE in year *t*

σ_t^I standard deviation of the estimate of observed CPUE in year *t*, obtained from the standardisation model

σ_t^{I2} standard deviation of the estimate of observed PCPUE in year *t*, obtained from the standardisation model

J_t standardised RDSI in year *t*

σ_t^J the standard deviation of the estimate of RDSI in year t, obtained from the standardisation model

$p_{k,t}^r$ observed proportion in the k^{th} length class in year *t* in RDLF

$p_{k,t}^s$ observed proportion in the k^{th} length class in year *t* in CSLF

l_j initial length for the j^{th} tag-recapture record

d_j observed length increment of the *j*th tag-recapture record

Δt_j time at liberty for the j^{th} tag-recapture record

p_k^{mat} observed proportion mature in the *k*th length class in the maturity dataset

2.2.4 Derived variables

R0 base number of annual recruits

$N_{k,t}$ number of paua in the k^{th} length class at the start of year *t*

$N_{k,t+0.5}$	number of paua in the k^{th} length class in the mid-season of year t
$R_{k,t}$	recruits to the model in the k^{th} length class in year t
g_k	expected annual growth increment for paua in the k^{th} length class
σ^{g_k}	standard deviation of the expected growth increment for paua in the k^{th} length class, used in calculating $\mathbf{G}$
$\mathbf{G}$	growth transition matrix
B_t	spawning stock biomass at the beginning of year t
$B_{t+0.5}$	spawning stock biomass in the mid-season of year t
B_0	equilibrium spawning stock biomass assuming no fishing and average recruitment from the period in which recruitment deviations were estimated.
B_{init}	spawning stock biomass at the end of initialisation phase (or B_{1964})
B_t^r	biomass of paua above the MLS at the beginning of year t
$B_{t+0.5}^r$	biomass of paua above the MLS in the mid-season of year t
B_0^r	equilibrium biomass of paua above the MLS assuming no fishing and average recruitment from the period in which recruitment deviations were estimated
B_{init}^r	biomass of paua above the MLS at the end of initialisation phase (or B_{1964}^r)
U_t	exploitation rate in year t
A_t	the complement of exploitation rate
$SF_{k,t}$	finite rate of survival from fishing for paua in the k^{th} length class in year t
V_k^r	relative selectivity of research divers for paua in the k^{th} length class
V_k^s	relative selectivity of commercial divers for paua in the k^{th} length class
$\sigma_{k,t}^r$	error of the predicted proportion in the k^{th} length class in year t in RDLF data
n_t^r	relative weight (effective sample size) of the RDLF data in year t
$\sigma_{k,t}^s$	error of the predicted proportion in the k^{th} length class in year t in CSLF data
n_t^s	relative weight (effective sample size)of the CSLF data in year t
σ_j^d	standard deviation of the predicted length increment for the j^{th} tag-recapture record
σ_j^{tag}	total error predicted for the j^{th} tag-recapture record
σ_k^{mat}	error of the proportion mature-at-length for the k^{th} length class
$-\ln(\mathbf{L})$	negative log-likelihood
f	total function value

2.2.5 Predictions

$\hat{I}_t$	predicted CPUE in year t
$\hat{I}2_t$	predicted PCPUE in year t
$\hat{J}_t$	predicted RDSI in year t
$\hat{p}_{k,t}^r$	predicted proportion in the k^{th} length class in year t in research diver surveys
$\hat{p}_{k,t}^s$	predicted proportion in the k^{th} length class in year t in commercial catch sampling

$\hat{d}_j$ predicted length increment of the j^{th} tag-recapture record

$\hat{p}_k^{mat}$ predicted proportion mature in the k^{th} length class

2.2.6 Initial conditions

The initial population is assumed to be in equilibrium with zero fishing mortality and the base recruitment. The model is run for 60 years with no fishing to obtain near-equilibrium in numbers-at-length. Recruitment is evenly divided among the first five length bins:

(1) $$R_{k,t} = 0.2R0 \qquad \text{for } 1 \le k \le 5$$

(2) $$R_{k,t} = 0 \qquad \text{for } k > 5$$

A growth transition matrix is calculated inside the model from the estimated growth parameters. If the growth model is linear, the expected annual growth increment for the *k*th length class is

(3) $$\Delta l_k = \left(\frac{\beta g_\alpha - \alpha g_\beta}{g_\alpha - g_\beta} - l_k \right) \left[1 - \left(1 + \frac{g_\alpha - g_\beta}{\alpha - \beta} \right) \right]$$

The model uses the AD Model Builder™ function *posfun*, with a dummy penalty, to ensure a positive expected increment at all lengths, using a smooth differentiable function. The *posfun* function is also used with a real penalty to force the quantity $\left(1 + \frac{g_\alpha - g_\beta}{\alpha - \beta} \right)$ to remain positive. If the growth model is exponential (used for the base case), the expected annual growth increment for the *k*th length class is

(4) $$\Delta l_k = g_\alpha \left(g_\beta / g_\alpha \right)^{(l_k - \alpha)/(\beta - \alpha)}$$

again using *posfun* with a dummy penalty to ensure a positive expected increment at all lengths.

The standard deviation of g_k is assumed to be proportional to g_k with minimum σ_{MIN} :

(5) $$\sigma^{g_k} = \left(g_k \phi - \sigma_{MIN} \right) \left(\frac{1}{\pi} \tan^{-1} \left(10^6 \left(g_k \phi - \sigma_{MIN} \right) \right) + 0.5 \right) + \sigma_{MIN}$$

From the expected increment and standard deviation for each length class, the probability distribution of growth increments for a paua of length l_k is calculated from the normal distribution and translated into the vector of probabilities of transition from the k^{th} length bin to other length bins to form the growth transition matrix **G**. Zero and negative growth increments are permitted, i.e., the probability of staying in the same bin or moving to a smaller bin can be non-zero.

In the initialisation, the vector $\mathbf{N_t}$ of numbers-at-length is determined from numbers in the previous year, survival from natural mortality, the growth transition matrix **G,** and the vector of recruitment $\mathbf{R_t}$:

(6) $$\mathbf{N_t} = \left(\mathbf{N_{t-1}} \, e^{-M} \right) \bullet \mathbf{G} + \mathbf{R_t}$$

where the dot (•) denotes matrix multiplication.

2.2.7 Dynamics

2.2.7.1 Sequence of operations

After initialising, the first model year is 1965 and the model is run through to 2010. In the first 9 years the model is run with an assumed catch vector, because it is unrealistic to assume that the fishery was in a virgin state when the first catch data became available in 1974. The assumed catch vector rises linearly from zero to the 1974 catch. These years can be thought of as an additional part of the initialisation, but they use the dynamics described in this section.

Model dynamics are sequenced as follows.

- Numbers at the beginning of year t-1 are subjected to fishing, then natural mortality, then growth to produce the numbers at the beginning of year t.
- Recruitment is added to the numbers at the beginning of year t.
- Biomass available to the fishery is calculated, and, with catch, is used to calculate the exploitation rate, which is constrained if necessary.
- Half the exploitation rate (but no natural mortality) is applied to obtain mid-season numbers, from which the predicted abundance indices and proportions-at-length are calculated. Mid-season numbers are not used further.

2.2.7.2 Main dynamics

For each year t, the model calculates the start-of-the-year biomass available to the commercial fishery. Biomass available to the commercial fishery is:

(7) $$B_t = \sum_k N_{k,t} V_k^s w_k$$

(8) $$V_k^{t,s} = \frac{1}{1+19^{-\left((l_k - D_{50}) / D_{95-50}\right)}} \qquad \text{for } t < 2007$$

(9) $$V_k^{t,s} = \frac{1}{1+19^{-\left((l_k - D_{50} - 5) / D_{95-50}\right)}} \qquad \text{for } t \geq 2007$$

The observed catch is then used to calculate exploitation rate, constrained for all values above U^{max} with the *posfun* function of AD Model Builder™. If the ratio of catch to available biomass exceeds U^{max}, then the exploitation rate is constrained and a penalty is added to the total negative log-likelihood function. Let minimum survival rate A_{min} be 1-U^{max} and survival rate A_t be 1-U_t:

(10) $$A_t = 1 - \frac{C_t}{B_t} \qquad \text{for } \frac{C_t}{B_t} \leq U^{\max}$$

$$(11)\qquad A_t = 0.5A_{\min}\left[1+\left(3-\frac{2\left(1-\frac{C_t}{B_t}\right)}{A_{\min}}\right)^{-1}\right] \quad \text{for } \frac{C_t}{B_t} > U^{\max}$$

The penalty invoked when the exploitation rate exceeds U^{max} is:

$$(12)\qquad 1000000\left(A_{\min} - \left(1-\frac{C_t}{B_t}\right)\right)^2$$

This prevents the model from exploring parameter combinations that give unrealistically high exploitation rates. Survival from fishing is calculated as:

$$(13)\qquad SF_{k,t} = 1-(1-A_t)P_{k,t}$$

or

$$(14)\qquad SF_{k,t} = 1-(1-A_t)V_k^s$$

The vector of numbers-at-length in year t is calculated from numbers in the previous year:

$$(15)\qquad \mathbf{N_t} = \left((\mathbf{SF_{t-1}} \otimes \mathbf{N_{t-1}})\mathrm{e}^{-M}\right)\bullet \mathbf{G} + \mathbf{R_t}$$

where $\otimes$ denotes the element-by-element vector product. The vector of recruitment, $\mathbf{R_t}$, is determined from $R0$ and the estimated recruitment deviations:

$$(16)\qquad R_{k,t} = 0.2R0e^{\left(\varepsilon_t - 0.5\sigma_\varepsilon^2\right)} \qquad \text{for } 1 \le k \le 5$$

$$(17)\qquad R_{k,t} = 0 \qquad \text{for } k > 5$$

The recruitment deviation parameters ε_t were estimated for all years from 1977; there was no constraint for deviations to have a mean of 1 in arithmetic space except for the constraint of the prior, which had a mean of zero in log space; and we assumed no stock recruitment relationship.

2.2.8 Model predictions

The model predicts CPUE in year t from mid-season recruited biomass, the scaling coefficient, and the shape parameter:

$$(18)\qquad \hat{I}_t = q^I\left(B_{t+0.5}\right)^h$$

Available biomass $B_{t+0.5}$ is the mid-season vulnerable biomass after half the catch has been removed (no natural mortality is applied, because the time over which half the catch is removed might be short). It is calculated as in equation (7), but using the mid-year numbers, $N_{k,t+0.5}$:

(19) $$N^{vuln}_{k,t+0.5} = N_{k,t}\left(1-\frac{(1-A_t)}{2}V^s_k\right).$$

Similarly,

(20) $$\hat{I}2_t = q^{I2}\left(B_{t+0.5}\right)^h = Xq^I\left(B_{t+0.5}\right)^h$$

The same shape parameter h is used for both series: experiment outside the model showed that this was appropriate despite the different units of measurement for the two series. The predicted research diver survey index is calculated from mid-season model numbers in bins greater than 89 mm length, taking into account research diver selectivity-at-length:

(21) $$N^{res}_{k,t+0.5} = N_{k,t}\left(1-\frac{(1-A_t)}{2}V^r_k\right)$$

(22) $$\hat{J}_t = q^J \sum_{k=11}^{55} N^{res}_{k,t+0.5}$$

where the scalar is estimated and the research diver selectivity V^r_k is calculated from:

(23) $$V^r_k = \frac{1}{1+19^{-\left((l_k-T_{50})/T_{95-50}\right)}}$$

The model predicts proportions-at-length for the RDLF from numbers in each length class for lengths greater than 89 mm:

(24) $$\hat{p}^r_{k,t} = \frac{N^{res}_{k,t+0.5}}{\sum_{k=11}^{51} N^{res}_{k,t+0.5}} \qquad \text{for } 11 \le k < 51$$

Predicted proportions-at-length for CSLF are similar:

(25) $$\hat{p}^s_{k,t} = \frac{N^{vuln}_{k,t+0.5}}{\sum_{k=23}^{51} N^{vuln}_{k,t+0.5}} \qquad \text{for } 23 \le k < 51$$

The predicted increment for the *j*th tag-recapture record, using the linear model, is

(26) $$\hat{d}_j = \left(\frac{\beta g_\alpha - \alpha g_\beta}{g_\alpha - g_\beta} - L_j\right)\left[1-\left(1+\frac{g_\alpha - g_\beta}{\alpha-\beta}\right)^{\Delta t_j}\right]$$

where Δt_j is in years. For the exponential model (used in the base case) the expected increment is

(27) $$\hat{d}_j = \Delta t_j g_\alpha \left(g_\beta / g_\alpha \right)^{\left(L_j - \alpha\right)/\left(\beta - \alpha\right)}$$

The error around an expected increment is

(28) $$\sigma_j^{\,d} = \left(\hat{d}_j \phi - \sigma_{MIN} \right) \left(\frac{1}{\pi} \tan^{-1} \left(10^6 \left(\hat{d}_j \phi - \sigma_{MIN} \right) \right) + 0.5 \right) + \sigma_{MIN}$$

Predicted maturity-at-length is

(29) $$\hat{p}_k^{mat} = \frac{1}{1 + 19^{-\left(\left(l_k - L_{50}\right) / L_{95-50} \right)}}$$

2.2.9 Fitting

2.2.9.1 Likelihoods

The distribution of CPUE is assumed to be normal-log and the negative log-likelihood is:

(30) $$-\ln(\mathbf{L})\left(\hat{I}_t \mid \theta \right) = \frac{\left(\ln\left(I_t\right) - \ln\left(\hat{I}_t\right) \right)^2}{2\left(\sigma_t^I \tilde{\sigma} / \varpi^I \right)^2} + \ln\left(\sigma_t^I \tilde{\sigma} / \varpi^I \right) + 0.5 \ln\left(2\pi\right)$$

and similarly for PCPUE:

(31) $$-\ln(\mathbf{L})\left(\hat{I}2_t \mid \theta \right) = \frac{\left(\ln\left(I2_t\right) - \ln\left(\hat{I}2_t\right) \right)^2}{2\left(\sigma_t^{I2} \tilde{\sigma} / \varpi^{I2} \right)^2} + \ln\left(\sigma_t^{I2} \tilde{\sigma} / \varpi^{I2} \right) + 0.5 \ln\left(2\pi\right)$$

The distribution of the RDSI is also assumed to be normal-log and the negative log-likelihood is:

(32) $$-\ln(\mathbf{L})\left(\hat{J}_t \mid \theta \right) = \frac{\left(\ln\left(J_t\right) - \ln\left(\hat{J}_t\right) \right)^2}{2\left(\sigma_t^J \tilde{\sigma} / \varpi^J \right)^2} + \ln\left(\sigma_t^J \tilde{\sigma} / \varpi^J \right) + 0.5 \ln\left(2\pi\right)$$

The proportions-at-length from CSLF data are assumed to follow a multinomial distribution, with a standard deviation that depends on the effective sample size (see Section 2.2.9.3) and the weight assigned to the data:

(33) $$\sigma_{k,t}^{s} = \frac{\tilde{\sigma}}{\varpi^s n_t^s}$$

The negative log-likelihood is:

$$(34) \qquad -\ln(\mathrm{L})\left(\hat{p}_{k,t}^{s} \mid \theta\right) = \frac{p_{s,t}^{s}}{\sigma_{k,t}^{s}}\left(\ln\left(p_{k,t}^{s} + 0.01\right) - \ln\left(\hat{p}_{k,t}^{s} + 0.01\right)\right)$$

The likelihood for research diver sampling is analogous. Errors in the tag-recapture dataset were also assumed to be normal. For the *j*th record, the total error is a function of the predicted standard deviation (equation (28)), observation error, and weight assigned to the data:

$$(35) \qquad \sigma_j^{tag} = \tilde{\sigma} / \varpi^{tag} \sqrt{\sigma_{obs}{}^{2} + \left(\sigma_j{}^{d}\right)^{2}}$$

and the negative log-likelihood is:

$$(36) \qquad -\ln(\mathbf{L})\left(\hat{d}_j \mid \theta\right) = \frac{\left(d_j - \hat{d}_j\right)^2}{2\left(\sigma_j^{tag}\right)^2} + \ln\left(\sigma_j^{tag}\right) + 0.5\ln\left(2\pi\right)$$

The proportion mature-at-length was assumed to be normally distributed, with standard deviation analogous to proportions-at-length:

$$(37) \qquad \sigma_k^{mat} = \frac{\tilde{\sigma}}{\varpi^{mat}\sqrt{p_k^{mat} + 0.1}}$$

The negative log-likelihood is:

$$(38) \qquad -\ln(\mathbf{L})\left(\hat{p}_k^{mat} \mid \theta\right) = \frac{\left(p_k^{mat} - \hat{p}_k^{mat}\right)^2}{2\left(\sigma_k^{mat}\right)^2} + \ln\left(\sigma_k^{mat}\right) + 0.5\ln\left(2\pi\right)$$

2.2.9.2 Normalised residuals

These are calculated as the residual divided by the relevant σ term used in the likelihood. For CPUE, the normalised residual is

$$(39) \qquad \frac{\ln\left(I_t\right) - \ln\left(\hat{I}_t\right)}{\left(\sigma_t^{I}\tilde{\sigma} / \varpi^{I}\right)}$$

and similarly for PCPUE and RDSI. For the CSLF proportions-at-length, the residual is

$$(40) \qquad \frac{p_{k,t}^{s} - \hat{p}_{k,t}^{s}}{\sigma_{k,t}^{s}}$$

and similarly for proportions-at-length from the RDLFs. Because the vectors of observed proportions contain many empty bins, the residuals for proportions-at-length include large numbers of small residuals, which distort the frequency distribution of residuals. When presenting normalised residuals from proportions-at-length, we arbitrarily ignore normalised residuals less than 0.05.

For tag-recapture data, the residual is

(41) $$\frac{d_j - \hat{d}_j}{\sigma_j^{tag}}$$

and for the maturity-at-length data the residual is

(42) $$\frac{p_k^{mat} - \hat{p}_k^{mat}}{\sigma_k^{mat}}$$

2.2.9.3 Dataset weights

Weights were chosen experimentally for each of the datasets, iteratively changing them to obtain standard deviations of the normalised residuals (*sdnr*) close to unity for each dataset.

Proportions at length (CSLF and RDLF) were included in the model with a multinomial likelihood. The length frequencies for individual years were assigned relative weights (effective sample sizes), based on a sample size that represented the best least squares fit of log(cv_i)~log(P_i), where cv_i was the bootstrapped c.v. for the *i*th proportion, P_i. Estimated and actual sample sizes for the commercial catch and research diver proportions at length for are given in Table 1Table 2 (see also Appendix A, Figures A1 & A2 for a plot of the relationship). The weights for individual years were further adjusted by the weight assigned to the dataset in the model.

2.2.9.4 Priors and bounds

Bayesian priors were established for all estimated parameters (Table 3). Most were incorporated simply as uniform distributions with upper and lower bounds arbitrarily set wide so as not to constrain the estimation. The prior probability density for M was a normal-log distribution with mean μ_M and standard deviation σ_M. The contribution to the objective function of estimated $M = x$ is:

(43) $$-\ln(\mathbf{L})(x \mid \mu_M, \sigma_M) = \frac{\left(\ln(M) - \ln(\mu_M)\right)^2}{2\sigma_M{}^2} + \ln\left(\sigma_M \sqrt{2\pi}\right)$$

The prior probability density for the vector of estimated recruitment deviations, ε, was assumed to be normal with a mean of zero and a standard deviation of 0.4. The contribution to the objective function for the whole vector is:

(44) $$-\ln\left(\mathbf{L}\right)(\varepsilon \mid \mu_\varepsilon, \sigma_\varepsilon) = \frac{\sum_{i=1}^{n_\varepsilon} \left(\varepsilon_i\right)^2}{2\sigma_\varepsilon{}^2} + \ln\left(\sigma_\varepsilon\right) + 0.5\ln\left(2\pi\right).$$

Constant parameters are given in Table 4.

2.2.9.5 Penalty

A penalty is applied to exploitation rates higher than the assumed maximum (equation 12); it is added to the objective function after being multiplied by an arbitrary weight (1E6) determined by experiment.

AD Model Builder™ also has internal penalties that keep estimated parameters within their specified bounds, but these should have no effect on the final outcome, because the choice of a base case excludes situations where parameters are estimated at or near a bound.

2.2.10 Fishery indicators

The assessment reports the following indicators calculated from their posterior distributions: the model's mid-season spawning and recruited biomass for 2010 ($B_{current}$ and $B^r_{current}$), for 2012 (B_{2012} and B^r_{2012}), and from the nadir (lowest point) of the population trajectory ($B_{\min}$ and $B^r_{\min}$).

The assessment reports B_{init} — the spawning stock biomass at the end of the initialisation phase (the equilibrium biomass assuming recruitment is equal to base recruitment and no fishing), and B_0 —the equilibrium spawning stock biomass assuming recruitment is equal to the average recruitment from the period for which recruitment deviation was estimated. B_0 will differ from B_{init} if the estimated average recruitment deviates from base recruitment (this will generally be true because the model has no constraint on the recruitment deviations aside from the priors). The ratio of $B_{current}$ to B_0 is a preferred indicator of current stock status (B_{init} was considered to have little biological meaning). The assessment also reports $B^r_{current}$, B^r_{init}, and B^r_0, being the current, initial, and virgin recruit-sized biomass respectively. The recruit-sized biomass is defined as paua above 125 mm, regardless of the changes of MHS.

2.2.11 Markov chain-Monte Carlo (MCMC) procedures

AD Model Builder™ uses the Metropolis-Hastings algorithm. The step size is based on the standard errors of the parameters and their covariance relationships, estimated from the Hessian matrix.

For the MCMCs in this assessment we ran single long chains that started at the MPD estimate. The base case was 5 million simulations long and we saved every 5000th samples. We fixed the value of σ to that used in the MPD run because it may be inappropriate to let a variance component change during the MCMC.

2.2.12 Initial, base case and sensitivity model runs

An initial model run (referred to as model 1.0) was firstly carried out. The initial run used model specifications as described above, and included

- a catch vector estimated under the base case assumption (40% of the commercial catch in Statistical Area 030 was taken from PAU 5A annually between 1985 and 1996)
- a standardised CPUE series based on CELR data from Statistical Areas 031 and 032 between 1990 and 2001
- a standardised CPUE series based on PCELR data between 2002 and 2009
- a standardised research diver survey index for 2002, 2006, and between 2008 and 2010

- a research diver survey proportions-at-lengths series for 1991, 2006, 2008–2010
- a commercial catch sampling length frequency series for 2002–2005
- tag-recapture length increment data
- maturity-at-length data.

The exponential growth model was used to fit the tag-recapture. Recruitment deviations were estimated for 1982–2006. The commercial fishing selectivity was shifted by 2 mm from 2007. The shape parameter *h* of the CPUE is fixed at 1. The relative weights for each dataset were adjusted iteratively until the standard deviations of the normalised residuals were close to 1.0 for each dataset (referred to as natural weights).

The results from the initial run suggested that the recent CPUE series (2002–09) were poorly fitted (see Section 3.1). A number of sensitivity runs were therefore carried out to investigate the effect on the model performance from various datasets. Model 1.1 estimated recruitment deviations only from 1992 to 2006; Model 2.0 excluded the early CPUE series; model 3.0 down-weighted the CSLF data and fixed the weights of other datasets at values from the initial run; model 3.1 excluded The CSLF and used natural weights for other datasets; model 4.0 down-weighted the RDLF data and fixed the weights of other datasets; model 4.1 excluded the RDLF and used natural weights for other datasets.

These sensitivity runs suggested that the model estimates were largely driven by the length frequency data rather than CPUE, and there appeared to be some conflicts between the RDLF and the recent CPUE series (see Section 3.1). Following the SFWG discussions, a base case model was chosen in which the recent CPUE series was up-weighted (model 5.0). An alterative model (8.0) was also proposed in which the shape parameter of CPUE (*h*) was estimated, allowing the relationship between CPUE and abundance to be non-linear (hyperstability model).

Additional sensitivity trials were also conducted. Models 5.1 and 5.2 are the same as the base case but used alternative catch history estimates (see figure 6 of Fu et al. 2010). The impacts of alternative fishing selectivity shifts of 3 and 4 mm were assessed for both the base case (6.1 and 6.2), and the hyperstability model (8.1 and 8.2). Table 5 provides a summary of the model runs described above.

3. RESULTS

3.1 MPD initial model run

Model estimates of objective function values (negative log-likelihood), parameters, and indicators for the initial run (1.0), base case (5.0), and sensitivity trials are given in Table 6.

The initial model fits well to the early CPUE indices (1990–2001), although it shows an opposite trend to the observed indices for the last few years of the series (Figure 2–top). The fits to the recent CPUE indices (2002–09) are not satisfactory and the model shows a much steeper decline than the observed CPUE (Figure 2–middle). The model fits poorly to the RDSI data and is unable to explain the inter-annual changes in the observed indices, although it shows a similar declining trend overall (Figure 2–bottom).

The fits to the commercial proportions-at-length has missed the mode of the length distribution for 2003 and 2005 (Figure 3), and slightly overestimated the proportions of large paua for 2004 and 2005 (Figure 4), but overall the fits are credible. The Fits to research diver proportions-at-length are reasonably good (Figure 5), and there is no consistent pattern between the residuals and length (Figure 6).

The QQ plots of the residuals show no apparent departure from the normal assumption (Figure 7). The weights chosen gave standard deviations of normalised residuals that were very close to 1 for all data set (Table 6). The standard deviations associated with the data encompassed the observational error, the common error term ($\tilde{\sigma}$), and the weight (see Section 2.2.9.3). For the early CPUE data the resulting standard deviations are half of the observed error; for the recent CPUE data, they are twice as much as the observed error. For the RDLF data, the model sample sizes are about 3 times more than the effective sample sizes; for the CSLF data, they are about 20% less.

The MPD estimate of M was 0.159, which is higher than the assumed mean of the prior distribution, 0.10. Estimates of maturity ogives were sensible, with length at 50% and full maturity estimated to be about 92 and 110 mm (Figure 8). Estimates of growth parameters suggested a mean annual growth of 25 mm at 75 mm and 6.9 mm at 120 mm, with a c.v. of about 0.23. The estimated growth transition matrix appeared to have accounted for most of the variability in the growth data (Figure 9).

The midpoint of the research diver selectivity ogive was 116 mm, and the ogive was broad (Figure 10). The midpoint of the commercial fishery selectivity was 126.3 mm, just slightly above the MLS, and this ogive was very narrow (Figure 10).

The model's MPD estimates of recruitment were lower than average in the early 1980s and above average through the 1990s (Figure 11).

The MPD estimates for the spawning stock biomass (mature animals) and recruited biomass (animals at or above the MLS) are shown in Figure 12. Both recruited and spawning biomass decreased from 1965, increased through most of the 1990s, and since then have declined substantially. $B_{current}$ is estimated to be about 28% of B_0, and $B^r_{current}$ is estimated to be about 17% of B^r_0 (Table 6, Figure 13)

3.2 MPD sensitivity trials and base case

Model 1.1 estimated recruitment deviations from 1992 to 2006, 10 years less than those estimated in the initial model. The RDLF sample from 1991 was excluded and the first length frequency available to this model is from 2002. The results suggested that estimated recruitment deviations for 1992–2006 were mostly similar to those of the initial model (Figure 14–left). The model fits the early CPUE indices slightly worse, showing a relatively flat trend (Figure 14–right). This is expected as recruitment deviations before 1990 were fixed at 1. The fits to other datasets are similar to those of the initial model.

Model 2.0 excluded the early CPUE series, but results showed that this had little impact. Most estimated parameters are the same as the initial model (Table 6) and the predicted CPUE indices (1990–2001) remain virtually unchanged (Figure 15). Further investigations suggested that exclusion of either the late CPUE or the RDSI had no effect on model results either. This implies that the model is mostly driven by the length frequency data.

Model 3.0 down-weighted the CSLF (an arbitrarily chosen weight of 0.05 was assigned) and weights for other datasets were fixed at values from the initial model run. Model 3.1 excluded the CSLF and weights for other datasets were determined using iterative re-weighting. For both models, fits to the CSLF are only marginally different from the initial model, and fits to other data and model estimates are similar (Figure 16, Table 6)

When the RDLF were down-weighted (4.0) or excluded (4.1), the fits to the RDLF were worse (Figure 17), but the fits to the recent CPUE were improved. There were also apparent changes in the estimates of recruitment deviations in the early part of the series (Figure 17).

Results from the above model runs indicated some inconsistency between the RDLF and the recent CPUE. To reconcile this conflict, a base case (5.0) was chosen in which the recent CPUE were up-weighted; a weight of 0.30 was assigned. This has the effect of reducing the standard deviations of the CPUE by 25%. Compared to the initial run, the base case improved the fits to the recent CPUE, with little or no effects on the fits to other observations (Figure 18). The estimated B_0 is close to the initial model, but the biomass declined more slowly in recent years, in line with the observed CPUE. $B_{current}$ is estimated to be about 41% of B_0 (Figure 19).

Model 8.0 estimated the shape parameter of the CPUE, *h*, to be 0.36, suggesting that the abundance declines much faster than the CPUE (hyperstability). The model also improved the fits to recent CPUE (Figure 18), but the biomass trajectory is very similar to that the initial model, with $B_{current}$ estimated to be about 25% of B_0. (Figure 19)

Models 5.1 and 5.2 included the upper and lower bound catch history estimates respectively, based on the base case model. The results are not significantly different from the base case (Table 6). $B_{current}$ was estimated to be 36% of B_0 for model 5.1, and 43% of B_0 for model 5.2.

In general, most estimated biological parameters were similar between the initial, base case, and sensitivity model runs. Estimates of natural mortality ranged from 0.132 to 0.189 for these models.

3.3 MCMC results

MCMC simulations were conducted for the base case and the hyperstability model. Both have assumed a shift of commercial fishing selectivity by 2 mm from 2007 onwards. MCMC simulations were also conducted assuming a shift of selectivity by 3 and 4 mm for each model (Models 6.1, 6.2, 8.1, and 8.2, see Table 5). The main diagnostics are shown for the base case using the trace and autocorrelation plots of the posterior samples (Figure 20). The MCMC traces showed good mixing and there is no excessive autocorrelation within the sampled chain for all the estimated parameters and indicators. In general, there is no obvious evidence that the chain is not converged. The MCMC parameter correlation matrix (Table 7) shows a high correlation between recruitment and *M*, as is usually seen; between the c.v. of growth and the other two growth parameters; between the two research diver selectivities; the two commercial selectivity parameters; and between the abundance scalars and one of the growth parameters. This list does not seem excessive.

3.4 Marginal posterior distributions and the Bayesian fit

Posteriors (Figure 20) for all estimated parameters and indicators were generally well formed and MPDs were mostly near the centrals (but tended to be below the median of biomass posteriors). Posteriors of the SDNRs were mostly in the range from 0.8 to 1.2 except for the recent CPUE as this dataset was upweighted. The posteriors are summarised in Table 8.

The posteriors of fits to CPUE appear to be adequate, though in some years have predictions that do not encompass the observed values (Figure 21). The posteriors of fits suggested that the model was unable to reproduce the range of variation seen in the RDSI data (Figure 22). The posteriors of fits to CSLF and RDLF were very reasonable, except for 2010 where larger paua were predicted (Figure 23).

The posteriors of selectivities are tight (Figure 23–top). Median recruitment is also similar to the MPD, but individual estimates show some level of uncertainty (Figure 23–middle). Exploitation rates are generally below 0.4 but are variable (Figure 23–bottom). The exploitation rate has increased since the mid 1990s, and remained at relatively high levels over the last few years.

Estimates from the base case suggest that the spawning stock population in 2010 (B_{current}) is 41% (34–50%) B_0, and recruit-sized stock abundance ($B^r_{cureent}$) is 26% (21–33%) of initial state (B^r_0). Estimates from the hyperstability model suggest that B_{current} is 26% (21–35%) B_0, and $B^r_{cureent}$ is 16% (12–22%) of B^r_0 (Table 10). Assuming larger selectivity shifts from 2007 generally led to more optimistic estimates of stock status. With a selectivity shift from 2 to 4 mm, the median of B_{current} (%B_0) ranged from 41% to 50% for the base case (Figure 24), and from 26% to 30% for the hyperstability model (Figure 25).

The projection made for the base case, assuming current catch levels and using recruitments re-sampled from the recent estimates, suggested that the stock abundance will decrease slightly over the next two years. The projected spawning stock biomass in 2012 has a median of 40% of B_0, about 3% less than the current level (Table 10). The probability that the spawning stock biomass will increase in two year's time (Pr{ $B_{2012} > B_{current}$ }) is about 22%. The hyperstability model predicted a larger decline in abundance, with B_{2012} predicted to be 6% less than the current state (Table 10). Projections made with alternative future catches suggested that Pr{ $B_{2012} > B_{current}$ } will increase with reduced catch levels. For the base case, Pr{ $B_{2012} > B_{current}$ } will be greater than 50% if the catch is reduced by 10 t each year for the next two years; for the hyperstability model, catch shelving of up to 20 t each year is needed. Projections made with larger selectivity shifts have all predicted declines in future stock abundance, but generally with smaller risks.

4. DISCUSSION

Assessments of New Zealand paua stocks have previously been conducted at the Quota Management Area level, as the fishery management decisions are usually made at these scales. For PAU 5A, there were concerns about the applicability of the assessment to the entire QMA, although there was general agreement that biomass decline had occurred in the southern region of the QMA over recent years. If abundances changes have differed between subareas, a QMA-level model assuming a homogenous area is unlikely to be informative regarding the stock status.

There have been changes in management initiatives in recent years towards fine-scale management of paua stocks. Subarea management zones, based on the research strata, have been established in PAU 5A since 2006, with a voluntary catch limit and minimum harvest size in place for each zone. Therefore a subarea level assessment is probably more relevant in informing management decisions. In addition, improvement of the collection and reporting of fishery data at finer scales has allowed the development of models to assess the fish stock at a smaller spatial scale.

This assessment is for the northern subarea of PAU 5A (Milford, George, Central, and Dusky). Although the choice of areas to be assessed was tentatively based on the availability of data, this could serve as a stepping-stone towards more fine-scale assessment in the future, in line with the refinement of data collection and the establishment of finer scale fishery management.

Results from the initial model suggested conflicts between the RDLF and the recent CPUE. Two models were proposed to reconcile the conflict: a base case in which the recent CPUE was up-weighted, and an alternative model in which the relationship between CPUE and abundance was assumed to be hyperstable. Both models improved fits to the recent CPUE. The base case suggested that there is no immediate concern about the current stock status, with current spawning stock population (B_{current}) estimated to be 41% (34–50%) B_0. The hyperstability model suggested that the biomass is declining faster than the observed CPUE, and therefore had more pessimistic results, with B_{current} estimated to be 26% (21–35%) B_0.

As the increase of MHS in 2007 varied by area, a number of alternative fishing selectivity shifts were considered. Models assuming greater selectivity shifts led to more optimistic estimates of stock status. When the assumed selectivity shift ranged from 2 to 4 mm, the median B_{current} ranged from 41% to 50% for the base case, and from 26% to 30% of B_0 for the hyperstability model. An attempt to estimate the selectivity change by incorporating the additional CSLF data between 2006 and 2010 was unsuccessful, as the distribution of sampling effort was patchy and had changed over time (see table 9 of Fu et. al. 2010).

The model projections made for the next two years, assuming current catch levels and using recruitments re-sampled from the recent model estimates, suggested the stock abundance will continue to decline slightly. For the base case, the projected spawning stock biomass in 2012 has a median of 41% of B_0 (3% less than the current level), and for the hyperstability model, B_{2012} has a median of 25% of B_0 (6% less than the current level).

The model presented here, whilst fairly representing some of the data, also shows some indications of lack of fit. It is unlikely the estimates of historical stock size are reliable, given assumptions about annual recruitment and the use of the historical catch-effort as an index of abundance.

We made no attempt to compare the results from this study with the previous assessment for several reasons, apart from the fact that a smaller area is covered in this assessment. Firstly, the revised catch history for PAU 5A is considerably different from previous assessments (see section 3 of Fu et. al. 2010). Secondly, separate CPUE and PCPUE indices are used whereas a combined CELR/PCELR series was used previously. Thirdly, the method for calculating research diver survey indices has been revised slightly. Fourthly, only four years of commercial catch sampling series are included.

The estimates of length-at maturity and growth parameters were similar to those from the southern area assessment (Fu & McKenzie 2010) as the same data were used. The estimated cv of the growth curve (ϕ) was much smaller in this assessment. One explanation was that the growth data were integrated within the model and estimates are also influenced by other observational data. MPD estimates of M were 0.135–0.189, generally higher than those from the southern area models (0.11–0.17), but appeared to be within the range seen in other assessments (Breen & Kim 2004b, McKenzie & Smith 2009).

Although the assessment is conducted at a smaller spatial scale, the model treats the whole of the assessed northern area of PAU 5A as if it were a single stock with homogeneous biology, habitat, and fishing pressures. This means that the model assumes homogeneity in recruitment, that natural mortality does not vary by size or year, and that growth has the same mean and variance throughout the area (paua fisheries are extremely variable and paua populations can change in very short distances along the coast). Heterogeneity in growth can be a problem for this kind of model (Punt 2003). Variation in growth is addressed to some extent by having a stochastic growth transition matrix based on increments observed in several different places; similarly the length frequency data are integrated across samples from many places.

The effect is likely to make model results optimistic. For instance, if some local stocks are fished very hard and others not fished, recruitment failure can result because of the depletion of spawners, because spawners must breed close to each other and because the dispersal of larvae is unknown and is thought to be limited. Recruitment failure is a common occurrence in overseas paua fisheries; local processes may therefore decrease recruitment, which is an effect that the current model cannot account for. Another concern is that the model could overestimate productivity in the population as a whole if fishing has caused spatial contraction of populations (e.g., Shepherd & Partington 1995) if some populations become relatively unproductive after initial fishing (Gorfine & Dixon 2000).

The commercial catch before 1974 is unknown and, although we think the effect is minor, major differences may exist between the catches we assume and what was taken. In addition, noncommercial catch estimates are poorly determined and could be substantially different from what was assumed. Estimates of illegal catch are not likely to be very reliable.

Uncertainty in the estimated catch history and its influence on the assessment has not been addressed in previous stock assessments of PAU 5A. The results from the 2010 southern area assessment (Fu & McKenzie 2010) suggested that estimates of stock status are sensitive to the range of assumptions made for the estimated catch history. For the northern area of PAU 5A, the commercial catch history is well determined back to 1984, although uncertainty exists for the pre-1984 catch (commercial catches are known with certainly back to 1995 for the southern area), and model fits and estimates of stock status are not significantly influenced by the alternative assumptions made on the early part of the catch history.

CPUE provides information on changes of relative abundance. However, CPUE is generally considered to be a poor index of stock abundance for paua, due to divers' ability to maintain catch rates by moving from area to area despite a decreasing biomass (hyperstability). The northern area of PAU 5A was generally thought to have been fished lightly in the early years as effort was more focused in the south. Through the 1990s, some old vessels were replaced by more powerful ones, and faster and larger tenders were deployed to allow fishers to gain better access to paua habitat. The increasing trend through the early CPUE therefore may have reflected improved fishing practice rather than changes in abundance. The declining trend in the later CPUE might have reflected a decline in abundance as the fishery was further developed. Attempts to estimate the relationship between CPUE and biomass (through the parameter h) have suggested evidence of hyperstability. The model showed that the biomass was declining faster than the observed CPUE in recent years, but increasing more than the observed CPUE through the 1990s, which seems unlikely.

Commercial catch length frequencies provide information on changes in population structure under fishing pressure. However, if serial depletion had occurred and fishers had moved from area to area, samples from the commercial catch may not have represented the population of the entire stock. Only four years of catch sampling (2002–05) were considered to be adequate for this assessment, and the sampling coverage has been low since then and is unreliable before 2002. It is anticipated that the sampling coverage will be improved in the future.

MPD fits to RDSI fit are generally poor, but this is expected as the RDSI is an imprecise measure and there is high variability between sites. The usefulness of research diver survey indices in providing relative abundance information has been an ongoing concern. Cordue (2009) concluded that the diver survey based on the timed swim approach is fundamentally flawed and is inadequate for providing relative abundance indices. A current review of survey methodology is underway and the preliminary results suggest that the existing RDSI data are likely to be more useful at stratum level. The general consensus is the index-abundance relationship from the research diver survey is likely to be nonlinear, and can not be easily quantified in a stock assessment.

Model fits to the length frequencies from the research diver surveys were reasonable, though structures existed in some years. Cordue (2009) suggested that RDLF are probably more useful at individual stratum level. The RDLF combined across strata may not be able to represent the underlying population at larger scale as the weight of individual strata can not be determined.

The growth was estimated from combined tag-recapture and isotopic increment data using an integrated approach. Model fits to growth data appeared adequate. However, it is unknown how accurate the growth estimates are. The data may not reflect fully the average growth and range of growth in this population. The differences in observational error between tag-recapture and isotopic experiments have not been accounted for in the model. For some stocks, such as PAU 5B (Breen et al. 2003), the modelled stock status was sensitive to the growth estimates, depending on the choice of data or the modelling approach. The growth parameters can be better determined if more and accurate growth data can be collected.

It is not known how well recruitment deviations were estimated. Breen et al. (2003) suggested that the actual recruitment fluctuations could be more extreme than those models suggested, as it takes a few years for paua to recruit into the fishery, and a strong pulse of year-class strengths could cover a wide length range. The recruitment deviations before 1992 are unlikely to be well estimated as there are few data to provide the information (the RDLF data are not continuous and there is a 10-year gap between the first and second length frequencies). Assuming constant recruitment before 1992 did not significantly change estimates of stock status, but made the fits to CPUE slightly worse.

There were some concerns over the iterative re-weighting procedure which was used to determine the relative weights for each dataset in the assessment model. The procedure is aimed to encourage the model to fit most datasets equally well. But the downside of this procedure is that model error could be unrealistically low for some datasets (e.g., the model sample size for RDLF in the base case is larger that the actual number of paua measured). There is also the risk that the level of uncertainty for some datasets may not be credibly quantified, particularly in the MCMC, and that the model results are more precise than they should be.

5. ACKNOWLEDGMENTS

This work was supported by a contract from the Ministry of Fisheries (PAU2007-04 Objective 1). Thank you to Paul Breen for developing the stock assessment model that was used in this assessment and for the use of major proportions of the 2006 report for this update. Reyn Naylor, NIWA, reviewed the manuscript.

6. REFERENCES

Andrew, N.L.; Breen, P.A.; Naylor, J.R.; Kendrick, T.H.; Gerring, P. (2000). Stock assessment of paua (*Haliotis iris*) in PAU 7 in 1998–99. *New Zealand Fisheries Assessment Report 2000/49*. 40 p.

Breen, P.A.; Andrew, N.L.; Kendrick, T.H. (2000a). Stock assessment of paua (*Haliotis iris*) in PAU 5B and PAU 5D using a new length-based model. *New Zealand Fisheries Assessment Report 2000/33*. 37 p.

Breen, P.A.; Andrew, N.L.; Kendrick, T.H. (2000b). The 2000 stock assessment of paua (*Haliotis iris*) in PAU 5B using an improved Bayesian length-based model. *New Zealand Fisheries Assessment Report 2000/48*. 36 p.

Breen, P.A.; Andrew, N.L.; Kim, S.W. (2001). The 2001 stock assessment of paua (*Haliotis iris*) in PAU 7. *New Zealand Fisheries Assessment Report 2001/55*. 53 p.

Breen, P.A.; Kim, S.W. (2003). The 2003 stock assessment of paua (*Haliotis iris*) in PAU 7. *New Zealand Fisheries Assessment Report 2003/35*. 112 p.

Breen, P.A.; Kim, S.W. (2004a). The 2004 stock assessment of paua (*Haliotis iris*) in PAU 4. *New Zealand Fisheries Assessment Report 2004/55*. 79 p.

Breen, P.A.; Kim, S.W. (2004b). The 2004 stock assessment of paua (*Haliotis iris*) in PAU 5A. *New Zealand Fisheries Assessment Report 2004/40*. 86 p.

Breen, P.A.; Kim, S.W. (2005). The 2005 stock assessment of paua (*Haliotis iris*) in PAU 7. *New Zealand Fisheries Assessment Report 2005/47*. 114 p.

Breen, P. A.; Kim, S.W. (2007). The 2006 stock assessment of paua (*Haliotis iris*) stocks PAU 5A (Fiordland) and PAU 5D (Otago). *New Zealand Fisheries Assessment Report 2007/09*. 164 p.

Breen, P.A.; Kim, S.W.; Andrew, N.L. (2003). A length-based Bayesian stock assessment model for paua. *Marine and Freshwater Research 54(5):* 619–634.

Cordue, P.L. (2009). Analysis of PAU5A dive survey data and PCELR catch and effort data. Final report for SeaFIC and PauaMAC5. (Unpublished report held by the Ministry of Fisheries and SeaFIC.)

Fu, D.; McKenzie, A. (2010). The 2010 stock assessment of paua (Haliotis iris) for Chalky and South Coast in PAU 5A. *New Zealand Fisheries Assessment Report 2010/36.*

Fu, D.; McKenzie, A; Naylor, R. (2010). Summary of input data for the 2010 PAU 5A stock assessment. *New Zealand Fisheries Assessment Report 2010/35.*

Gorfine, H.K.; Dixon, C.D. (2000) A behavioural rather than resource-focused approach may be need to ensure sustainability of quota managed paua fisheries. *Journal of Shellfish Research* 19: 515–516.

Kim, S.W.; Bentley, N.; Starr, P.J.; Breen, P.A. (2004). Assessment of red rock lobsters (Jasus edwardsii) in CRA 4 and CRA 5 in 2003. *New Zealand Fisheries Assessment Report 2004/8.*

McKenzie, A.; Smith, A.N.H. (2009). The 2008 stock assessment of paua (*Haliotis iris*) in PAU 7. *New Zealand Fisheries Assessment Report 2009/34*. 84 p.

McShane, P.E. (1994). Estimating the abundance of stocks of paua *(Haliotis spp.*) – examples from Victoria and southern New Zealand. *Fisheries Research 19*: 379–394.

McShane, P.E.; Mercer, S.F.; Naylor, J.R. (1994). Spatial variation and commercial fishing of the New Zealand paua (*Haliotis iris* and *H. australis*). *New Zealand Journal of Marine and Freshwater Research 28*: 345–355.

McShane, P.E.; Mercer, S.; Naylor, J.R.; Notman, P.R. (1996): Paua (*Haliotis iris*) fishery assessment in PAU 5, 6, and 7. New Zealand Fisheries Assessment Research Document 96/11. 35 p. (Unpublished report held in NIWA library, Wellington.)

Ministry of Fisheries Science Group (2009). Report from the Fisheries Assessment Plenary, May 2009: stock assessments and yield estimates. Ministry of Fisheries. Wellington, New Zealand. 990 p.

Punt, A.E. (2003). The performance of a size-structured stock assessment method in the face of spatial heterogeneity in growth. *Fisheries Research 65:* 391–409.

Schiel, D.R. (1989). Paua fishery assessment 1989. New Zealand Fisheries Assessment Research Document 89/9. 20 p. (Unpublished report held in NIWA library, Wellington, New Zealand.)

Schiel, D.R. (1992). The paua (paua) fishery of New Zealand. *In* Paua of the world: Biology, fisheries and culture. Shepherd, S.A.; Tegner, M.J.; Guzman del Proo, S. (eds.) pp. 427–437. Blackwell Scientific, Oxford.

Schiel, D.R.; Breen, P.A. (1991). Population structure, ageing and fishing mortality of the New Zealand paua *Haliotis iris*. *Fishery Bulletin 89*: 681–691.

Shepherd, S.A.; Breen, P.A. (1992). Mortality in paua: its estimation, variability and causes. In 'Paua of the World: Biology, Fisheries and Culture'. Shepherd, S.A; Tegner,M.J.; Guzman del Proo, S. (eds.) pp. 276–304. Blackwell Scientific: Oxford.

Shepherd, S.A.; Partington, D. (1995). Studies on Southern Australian paua (genus Haliotis). XVI. Recruitment, habitat and stock relations. *Marine and Freshwater Research 46*: 669–680.

Shepherd, S.A.; Rodda, K.R.; Vargas, K.M. (2001). A chronicle of collapse in two paua stocks with proposals for precautionary management. *Journal of Shellfish Research 20*: 843–856.

Table 1: Actual sample sizes and effective sample sizes determined for the multinomial likelihood for the commercial catch proportions at length for Milford, George, Central, and Dusky combined. Note only the 2002–2005 observations were included in the assessment model.

Year	Actual sample size	Effective sample size
1992	3548	1076
1993	331	340
1998	370	292
2000	201	134
2001	245	131
2002	1775	1097
2003	1552	1933
2004	3610	1622
2005	1936	1156
2006	965	669
2007	1472	819
2008	2117	1123
2009	1113	443

Table 2: Actual sample sizes and effective sample sizes determined for the multinomial likelihood for the research diver survey proportions at length for Milford, George, Central, and Dusky combined for 1991, 2002, 2006, and 2008–2010.

Year	Actual sample size	Effective sample size
1991	1272	300
2002	1174	334
2006	988	369
2008	579	188
2009	1339	515
2010	1104	297

Table 3: Base case model specifications: for estimated parameters, the phase of estimation, lower bound, upper bound, type of prior, (U, uniform; N, normal; LN, lognormal), mean and c.v. of the prior.

Parameter	Phase	Prior	μ	c.v.	Bounds	
					Lower	Upper
			–	–		
ln($R0$)	1	U	–	–	5	50
M	3	LN	0.1	0.1	0.01	0.5
g_{α}	2	U			1	50
g_{β}	2	U			0.01	50
ϕ	2	U			0.001	1
$\ln(q^{I})$	1	U			-30	0
X	1	U			0.05	10
$\ln(q^{J})$	1	U			-30	0
L_{50}	1	U			70	145
L_{95-50}	1	U			1	50
T_{50}	2	U			70	125
T_{95-50}	2	U			0.001	50
D_{50}	2	U			70	145
D_{95-50}	2	U			0.01	50
ε	1	N	0	0.4	0.01	1

Table 4: Values for fixed quantities for base case model.

Variable	Value
α	75
β	120
a	2.99E-08
b	3
$U^{\max}$	0.65
σ_{MIN}	1.0
σ_{obs}	0.25
h	1
$\tilde{\sigma}$	0.2
ϖ^{I}	0.16
ϖ^{I2}	0.21
ϖ^{J}	0.23
ϖ^{r}	0.14
ϖ^{s}	0.21
ϖ^{tag}	0.14
ϖ^{mat}	3.85

Table 5: Summary descriptions for initial, base case, and sensitivity model runs.

Mode runs	Descriptions
1.0 (Initial run)	CSLF 2002–2005, estimated ε for 1982–2006, selectivity shifted by 2mm from 2007
1.1	Initial run, but dropped 1992 RDLF, and estimated ε for 1992–2006
2.0	Initial run, but excluded CPUE 1990–2001
3.0	Initial run, but down-weighted CSLF and fixed weights for other datasets
3.1	Initial run, but down-weighted CSLF and reweighted other datasets
4.0	Initial run, but down-weighted RDLF and fixed weights for other datasets
4.1	Initial run, but down-weighted RDLF and reweighted for other data
5.0 (base case)	Initial run, but up-weighted CPUE 2002–2009
5.1	Base case, but with the upper-bound catch estimates,
5.2	Base case, but with the lower-bound catch estimates
6.1	Base case, selectivity shifted by 3mm from 2007
6.2	Base case, selectivity shifted by 4mm from 2007
8.0 (hyperstability)	Initial run, but estimated shape parameter for CPUE
8.1	8.0, selectivity shifted by 3mm from 2007
8.2	8.0, selectivity shifted by 4mm from 2007

Table 6: MPD estimates for initial (1.0), base case (5.0), and sensitivity trials. *SDNR*s: standard deviations of the normalised residuals. Shading indicates *SDNR*s inflated because they were not estimated, likelihood contributions not used when datasets were removed, and parameter fixed at the base case estimates.

Model runs	1.0	1.1	2.0	3.0	3.1	4.0	4.1	5.0	5.1	5.2	6.1	6.2	8.0	8.1	8.2
Weights															
CPUE	0.36	0.25	0.37	0.37	0.38	0.37	0.31	0.37	0.38	0.37	0.37	0.37	0.34	0.32	0.31
PCPUE	0.10	0.10	0.10	0.10	0.10	0.10	0.26	0.30	0.30	0.30	0.3	0.3	0.22	0.23	0.23
RDSI	0.20	0.20	0.20	0.20	0.20	0.20	0.20	0.20	0.20	0.20	0.2	0.2	0.19	0.2	0.2
CSLF	0.15	0.15	0.15	0.01	0.03	0.15	0.15	0.15	0.15	0.15	0.15	0.15	0.15	0.15	0.15
RDLF	0.69	0.67	0.69	0.69	0.72	0.01	0.23	0.68	0.70	0.69	0.69	0.66	0.71	0.7	0.68
Tags	0.11	0.11	0.11	0.11	0.11	0.11	0.11	0.11	0.11	0.11	0.11	0.1	0.11	0.11	0.11
Maturity	3.85	3.85	3.85	3.85	3.85	3.85	3.85	3.85	3.85	3.85	3.85	3.85	3.85	3.85	3.85
sdnrs															
sdnrCPUE	0.97	1.01	1.47	0.96	0.99	1.13	1.01	1.03	1.03	1.05	1.04	1.05	1.00	1.00	1.01
sdnrPCPUE	1.03	1.03	1.01	0.98	0.98	0.55	0.99	1.57	1.62	1.55	1.60	1.67	0.99	0.99	0.97
sdnrRDSI	1.00	1.00	1.00	1.01	1.01	0.95	0.98	0.98	0.98	0.98	0.99	1.00	0.98	1.02	1.00
sdnrCSLF	1.00	1.00	0.99	0.30	0.52	0.97	0.98	1.01	1.01	1.01	1.01	1.01	1.00	0.99	0.99
sdnrRDLF	0.99	1.00	1.00	0.98	1.00	0.16	0.82	1.02	1.02	1.03	1.03	1.03	1.00	1.00	1.00
sdnrMaturity	1.00	1.00	1.00	1.00	1.00	1.00	1.00	1.00	1.00	1.00	1.00	1.00	1.00	1.00	1.00
sdnrTags	1.01	1.01	1.01	1.02	1.02	1.04	1.04	1.01	1.01	1.01	1.01	0.98	1.01	1.01	1.01
Likelihoods															
CPUE	-10.8	-5.8	118.3	-11.2	-11.2	-9.1	-8.5	-10.4	-10.8	-10.1	-10.3	-10.2	-9.7	-9.0	-8.5
PCPUE	-3.6	1.9	-3.8	-4.0	-4.1	-6.6	-11.6	-6.7	-6.2	-7.0	-6.5	-5.5	-10.3	-10.6	-10.7
RDSI	1.9	54.1	1.9	2.0	1.9	1.7	1.8	1.8	1.8	1.8	1.9	1.9	2.1	2.0	1.9
CSLF	53.6	117.1	53.4	4.9	14.4	51.7	52.0	54.9	54.9	55.1	55.1	55.5	53.7	53.6	53.6
RDLF	139.3	843.8	140.3	134.2	140.4	3.7	99.3	145.2	147.2	148.1	150.0	148.8	140.4	141.7	141.4
Tags	844.0	-16.7	844.0	843.9	844.1	844.1	844.2	844.4	844.1	844.6	844.3	843.1	844.3	844.0	843.9
Maturity	-16.7	-16.7	-16.7	-16.7	-16.7	-16.7	-16.7	-16.7	-16.7	-16.7	-16.7	-16.7	-16.7	-16.7	-16.7
Prior on M	9.4	2.6	9.4	10.1	10.7	3.1	3.1	15.7	10.5	18.9	17.6	19.0	8.5	9.1	10.1
Prior on ε	14.5	9.9	13.9	14.9	14.6	9.4	9.2	8.6	8.5	8.5	7.8	6.9	17.7	16.2	14.7
U penalty	0.0	0.0	0.0	0.0	0.0	0.0	0.0	0.0	0.0	0.0	0.0	0.0	0.0	0.0	0.0
Total likelihood	1031.6	1003.2	1042.3	978.0	979.8	877.6	873.7	1036.9	1033.4	1043.1	1043.2	1042.9	1030.0	1030.4	1029.8

Table 6–continued.

Parameters	1.0	1.1	2.0	3.0	3.1	4.0	4.1	5.0	5.1	5.2	6.1	6.2	8.0	8.1	8.2
ln(*R0*)	12.8	12.7	12.9	12.8	12.9	12.8	12.8	13.2	13.0	13.2	13.2	13.3	12.8	12.8	12.9
M	0.159	0.132	0.159	0.162	0.164	0.135	0.135	0.179	0.163	0.189	0.185	0.189	0.156	0.158	0.161
T_{50}	116.4	115.8	116.3	117.3	117.4	117.4	117.4	115.8	115.6	116.0	115.5	115.1	116.8	116.2	115.7
$T_{95\text{-}50}$	20.1	19.6	20.0	20.9	21.0	20.9	20.9	19.0	19.0	18.9	18.6	18.1	20.1	19.8	19.3
D_{50}	126.2	126.2	126.3	125.9	126.2	126.1	126.2	126.4	126.3	126.4	126.3	126.2	126.2	126.2	126.1
$D_{95\text{-}50}$	4.7	4.6	4.7	3.7	4.7	4.6	4.7	4.8	4.7	4.8	4.7	4.6	4.7	4.6	4.6
L_{50}	91.8	91.8	91.8	91.8	91.8	91.8	91.8	91.8	91.8	91.8	91.8	91.8	91.8	91.8	91.8
$L_{95\text{-}50}$	19.6	19.6	19.6	19.6	19.6	19.6	19.6	19.6	19.6	19.6	19.6	19.6	19.6	19.6	19.6
$\ln(q^I)$	-12.5	-12.5	-13.0	-12.5	-12.4	-12.6	-12.6	-12.7	-12.6	-12.7	-12.7	-12.8	-4.5	-4.1	-3.7
X	1.5	1.5	2.3	1.4	1.4	1.3	1.2	1.4	1.3	1.4	1.4	1.3	1.1	1.1	1.1
$\ln(q^J)$	-12.5	-12.5	-13.0	-12.5	-12.4	-12.6	-12.6	-12.7	-12.6	-12.7	-12.7	-12.8	-4.5	-4.1	-3.7
g_α	24.8	25.2	24.9	24.5	24.3	26.8	27.0	25.0	24.8	25.1	25.2	25.4	24.1	24.5	24.7
g_β	6.9	7.0	6.9	7.0	6.9	7.0	7.0	6.8	6.9	6.8	6.8	6.8	7.0	7.0	7.0
φ	0.23	0.22	0.23	0.22	0.22	0.21	0.21	0.23	0.23	0.23	0.23	0.21	0.23	0.23	0.23
Indicators															
B_0	984	1203	986	962	957	1070	1089	986	1016	978	993	1024	975	978	979
B_{init}	741	846	750	723	724	941	963	838	866	835	866	917	703	720	739
$B_{current}$	275	252	280	267	272	350	386	400	369	422	439	501	244	262	282
$B_{current}/B_0$	0.28	0.21	0.28	0.28	0.28	0.33	0.35	0.41	0.36	0.43	0.44	0.49	0.25	0.27	0.29
$B_{current}/B_{init}$	0.37	0.30	0.37	0.37	0.38	0.37	0.40	0.48	0.43	0.50	0.51	0.55	0.35	0.36	0.38
rB_0	799	1025	800	777	769	909	927	769	818	748	767	781	797	796	792
rB_{init}	601	721	608	584	582	800	819	653	697	639	669	699	575	586	598
$rB_{current}$	138	129	141	131	133	209	242	217	202	227	243	284	118	130	144
$rB_{current}/rB_0$	0.17	0.13	0.18	0.17	0.17	0.23	0.26	0.28	0.25	0.30	0.32	0.36	0.15	0.16	0.18
$rB_{current}/rB_{init}$	0.23	0.18	0.23	0.22	0.23	0.26	0.30	0.33	0.29	0.36	0.36	0.41	0.21	0.22	0.24
$U_{current}$	0.35	0.37	0.35	0.36	0.36	0.26	0.23	0.26	0.28	0.25	0.25	0.23	0.39	0.38	0.38

Table 7: Correlations among estimated parameters for the base case MCMC. Boxes indicate absolute values greater than 0.50.

Parameter	ln($R0$)	M	g_{α}	g_{β}	T_{50}	$T_{95\text{-}50}$	D_{50}	$D_{95\text{-}50}$	L_{50}	$L_{95\text{-}50}$	φ	ln(q^I)	X	ln(q^J)
ln($R0$)	1.00													
M	0.89	1.00												
g_{α}	-0.22	-0.17	1.00											
g_{β}	-0.21	0.15	0.21	1.00										
T_{50}	0.52	0.52	-0.37	-0.05	1.00									
$T_{95\text{-}50}$	-0.01	-0.03	0.04	-0.13	0.53	1.00								
D_{50}	0.12	0.12	-0.27	-0.02	0.17	0.02	1.00							
$D_{95\text{-}50}$	0.06	0.04	-0.14	-0.03	0.09	0.01	0.72	1.00						
L_{50}	0.00	0.00	0.00	0.00	0.00	0.00	0.00	0.00	1.00					
$L_{95\text{-}50}$	0.00	0.00	0.00	0.00	0.00	0.00	0.00	0.00	-0.33	1.00				
φ	0.13	-0.04	-0.27	-0.51	0.09	0.10	0.07	0.05	0.00	0.00	1.00			
ln(q^I)	-0.57	-0.35	-0.13	0.57	-0.10	-0.01	0.15	0.11	0.00	0.00	-0.22	1.00		
X	-0.05	-0.04	0.06	0.02	0.16	0.15	0.13	0.08	0.00	0.00	0.01	0.12	1.00	
ln(q^J)	-0.31	-0.20	-0.03	0.26	0.07	0.11	0.02	0.01	0.00	0.00	-0.10	-0.05	-0.31	1.00

Table 8 : Summary of the marginal posterior distributions from the MCMC chain from the base case. The columns show the minimum values observed in the 1000 samples, the maxima, the 5th and 95th percentiles, and the medians. Biomass is in tonnes.

	Min	5%	Median	95%	Max
SDNRs					
sdnrCPUE	0.93	0.99	1.08	1.25	1.47
sdnrCPUE2	1.08	1.27	1.57	1.92	2.31
sdnrRDSI	0.89	0.92	0.98	1.06	1.14
sdnrCSLF	0.99	1.01	1.04	1.08	1.13
sdnrRDLF	0.99	1.02	1.04	1.07	1.10
sdnrmat	0.88	0.92	0.98	1.04	1.09
sdnrtags	1.00	1.00	1.04	1.16	1.40
Parameters					
f	1046.0	1050.6	1057.6	1066.3	1076.6
ln($R0$)	12.76	12.96	13.18	13.40	13.63
M	0.14	0.16	0.18	0.20	0.22
T_{50}	112.13	114.12	115.67	117.38	119.16
$T_{95\text{-}50}$	14.27	17.09	19.38	21.92	24.05
D_{50}	125.57	125.96	126.34	126.73	127.07
$D_{95\text{-}50}$	3.82	4.18	4.77	5.40	5.96
L_{50}	87.97	89.95	91.64	93.18	94.96
$L_{95\text{-}50}$	12.27	16.23	20.03	24.62	29.74
ln(q^I)	-12.96	-12.85	-12.71	-12.58	-12.47
X	1.20	1.27	1.38	1.49	1.59
ln(q^J)	-14.61	-14.34	-14.05	-13.76	-13.48
g_α	21.70	23.42	25.48	27.70	30.57
g_β	6.06	6.35	6.69	6.99	7.42
φ	0.20	0.22	0.24	0.26	0.28
Indicators					
B_0	913	960	1012	1065	1123
B_{init}	727	782	858	961	1065
$B_{current}$	300	351	417	498	580
$B_{current}/B_0$	0.29	0.35	0.41	0.49	0.54
B_0^r	694	737	787	843	926
B_{init}^r	545	613	670	734	809
$B_{current}^r$	150	175	207	250	305
$B_{current}^r/B_0^r$	0.18	0.22	0.26	0.31	0.38
$U_{current}$	0.22	0.27	0.31	0.36	0.41

Table 9: Bayesian median and 95% credible intervals of B_0, B_0^r, $B_{2010}(\%B_0)$, and $B_{2010}^r(\%B_0^r)$ for MCMC base case and sensitivity runs.

Model	B_0 (t)	B^r(t)	B_{2010} (% B_0)	B^r_{2010} (% B^r_0)
5.0	1012 (949–1084)	787 (730–855)	41.3 (34.0–50.1)	26.4 (21.3–32.5)
6.1	1022 (960–1095)	789 (727–855)	45.1 (36.6–54.6)	29.6 (23.5–36.9)
6.2	1050 (979–1135)	801 (741–867)	49.8 (41.1–59.2)	30.4 (24.6–37.3)
8.0	989 (923–1065)	805 (727–887)	26.4 (20.5–34.7)	16.1 (11.8–22.3)
8.1	993 (927–1063)	803 (726–887)	28.2 (21.7–37.3)	17.6 (12.8–24.3)
8.2	992 (928–1062)	799 (731–884)	30.3 (23.7–39.2)	19.4 (14.4–26.3)

Table 10 : Bayesian median and 95% credible intervals of $B_{2012}(\%B_0)$ and $B_{2012}(\%B_{2010})$, and the probability that $B_{2012} > B_{2010}$ for MCMC projections for base case and sensitivity runs assuming various future catch levels.

Model	Catch	B_{2012} (% B_0)	B_{2012} (% B_{2010})	$Pr(B_{2012} > B_{2010})$
5.0	74 330	40.0 (31.8–49.5)	0.97 (0.89–1.05)	0.218
	69 330	40.7 (32.5–50.2)	0.99 (0.91–1.06)	0.364
	64 330	41.4 (33.2–50.8)	1.00 (0.93–1.08)	0.520
6.1	74 330	43.9 (34.4–54.1)	0.97 (0.90–1.05)	0.249
	69 330	44.6 (35.1–54.7)	0.99 (0.92–1.06)	0.369
	64 330	45.3 (35.8–55.3)	1.00 (0.94–1.08)	0.550
6.2	74 330	48.9 (39.8–60.0)	0.98 (0.92–1.05)	0.312
	69 330	49.6 (40.5–60.6)	0.99 (0.94–1.07)	0.434
	64 330	50.3 (41.2–61.2)	1.01 (0.95–1.08)	0.607
8.0	74 330	24.7 (19.1–33.3)	0.94 (0.82–1.06)	0.140
	64 330	25.4 (19.1–34.7)	0.97 (0.85–1.07)	0.278
	54 330	26.8 (19.7–36.1)	1.01 (0.89–1.12)	0.598
8.1	74 330	26.4 (19.9–35.6)	0.94 (0.83–1.06)	0.17
	64330	27.2 (20.1–37.1)	0.97 (0.86–1.08)	0.329
	54330	28.6 (20.6–38.5)	1.02 (0.90–1.12)	0.638
8.2	74 330	28.5 (22.3–37.8)	0.95 (0.84–1.05)	0.165
	64 330	28.5 (22.3–37.8)	0.98 (0.88–1.07)	0.361
	54 330	28.5 (22.3–37.8)	1.02 (0.92–1.11)	0.671

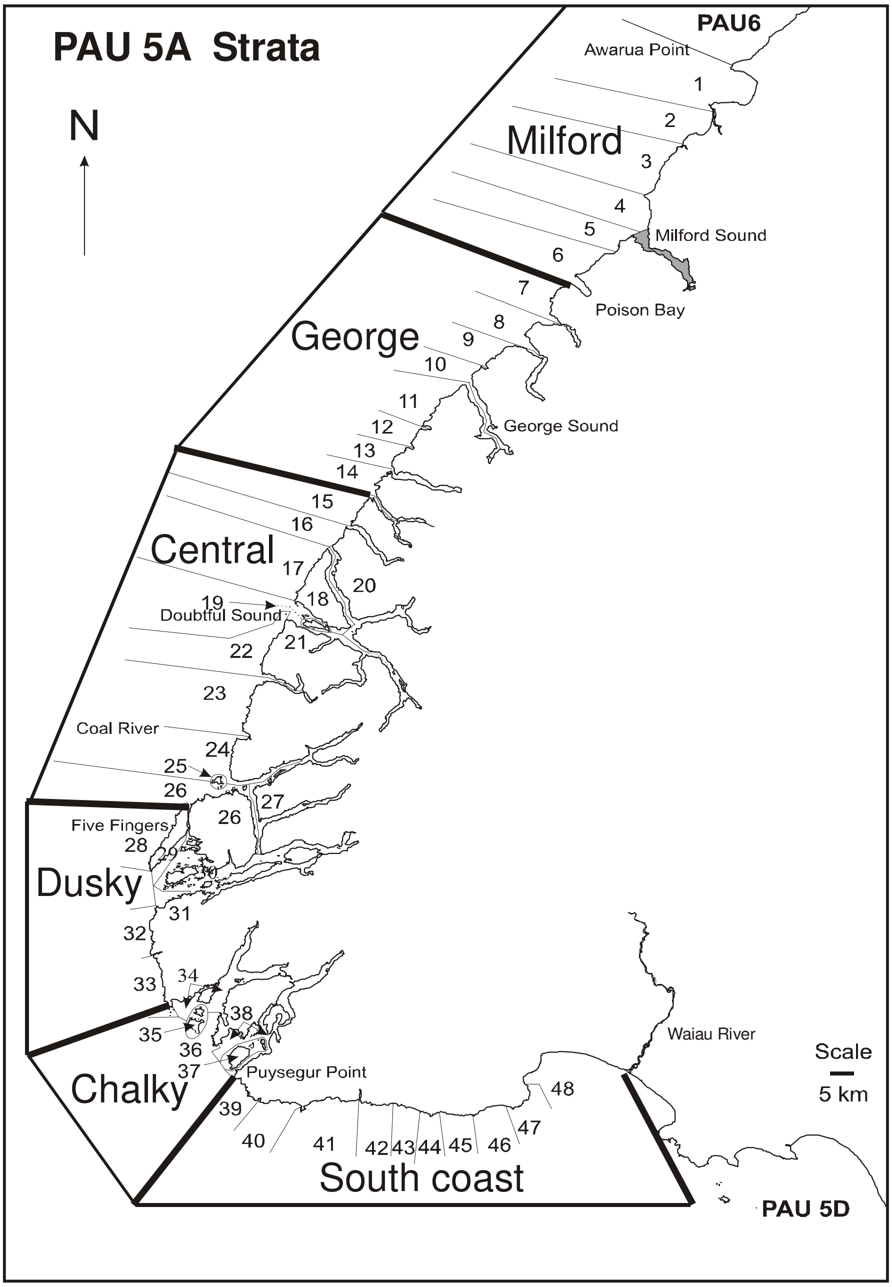

Figure 1: Boundaries of PAU 5A, fine-scale statistical area and research survey strata.

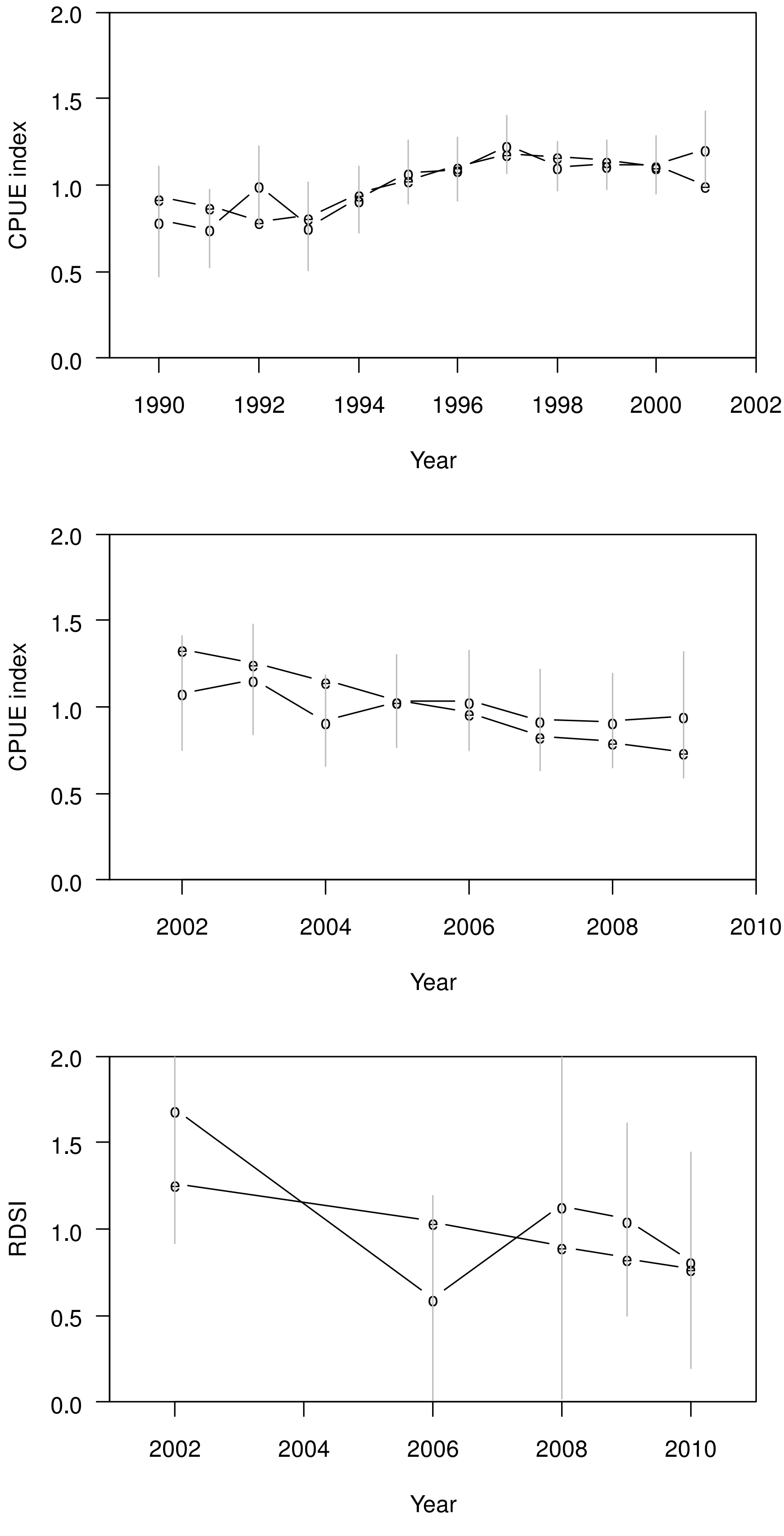

Figure 2: Observed (dots) and predicted (solid line) CPUE (top), PCPUE (middle), and RDSI (bottom) for the initial model MPD fit. Error bars show the standard error term used by the model in fitting, including the effects of the common error term and the dataset weights.

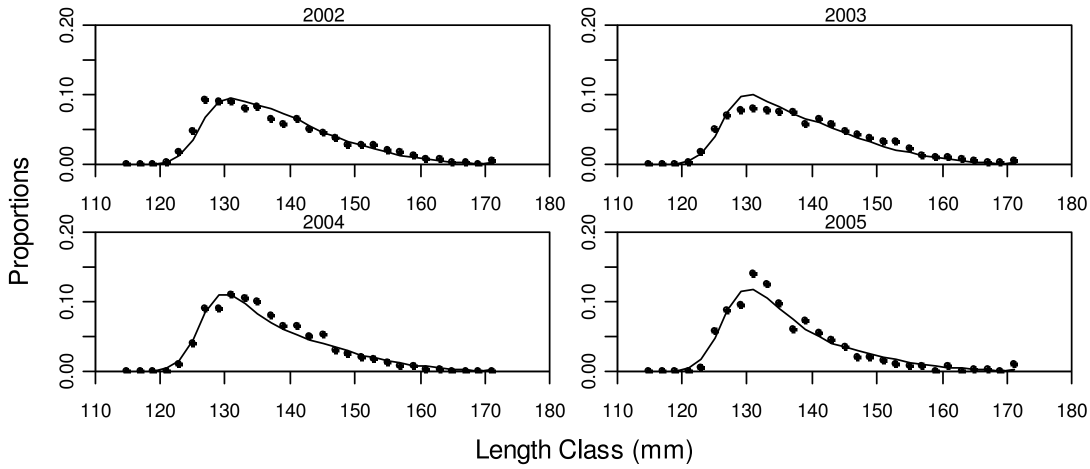

Figure 3: Observed (dots) and predicted (lines) proportions-at-length from commercial catch sampling (CSLF) for the initial model (1.0) MPD fit.

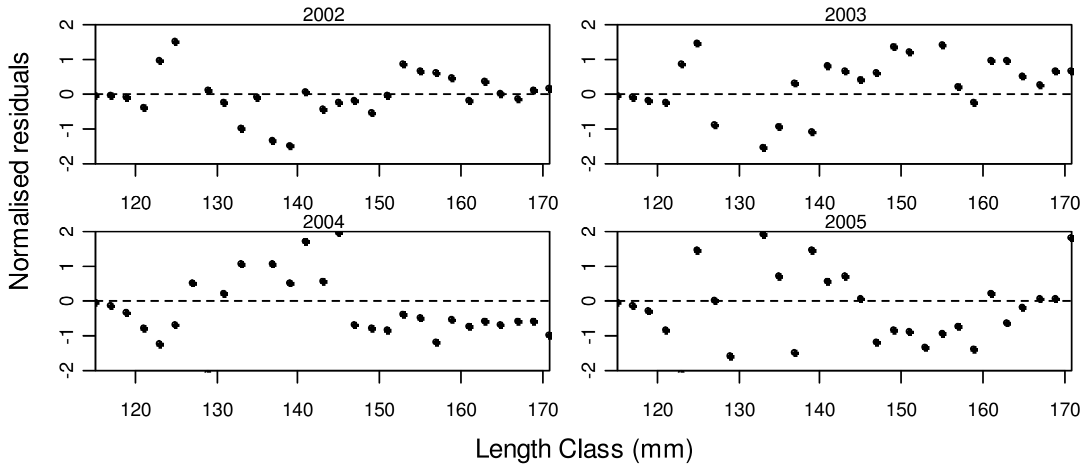

Figure 4: Residuals from the initial model MPD fits to CSLF data seen in Figure 3.

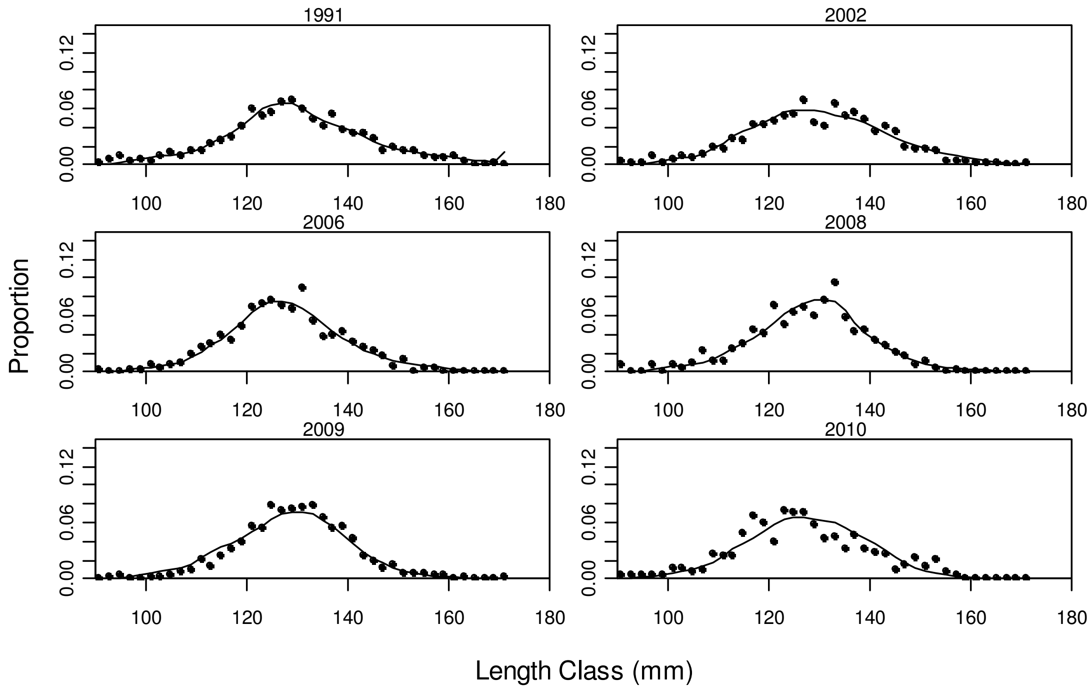

Figure 5: Observed (dots) and predicted (lines) proportions-at-length from research diver survey catch sampling (RDLF) for the initial model MPD fit.

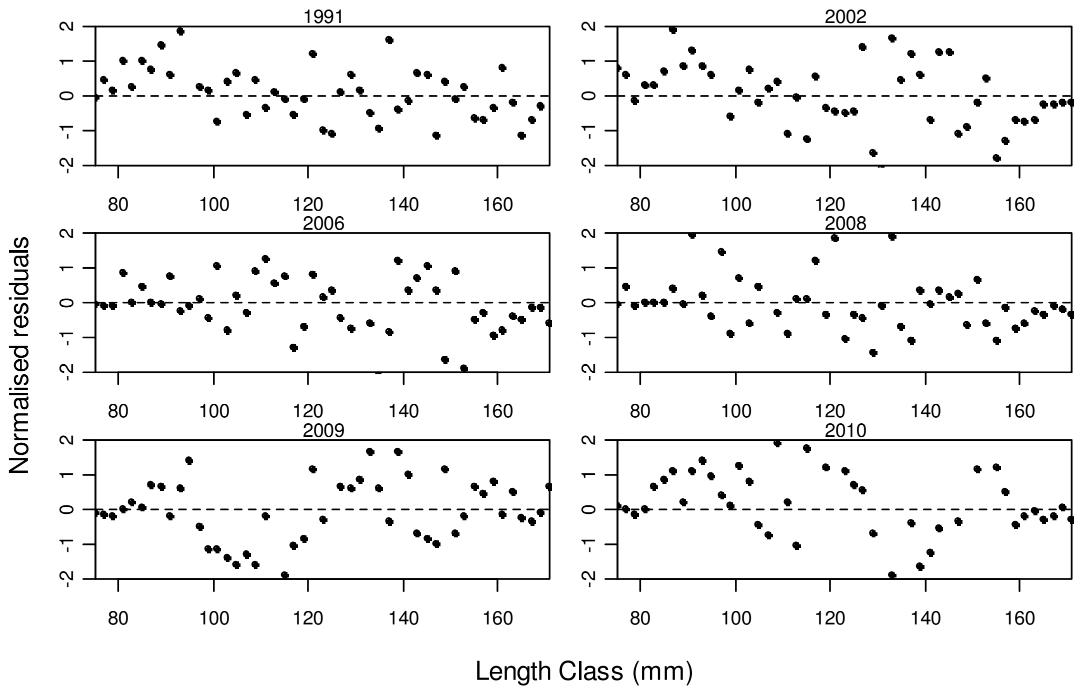

Figure 6: Residuals from the initial model MPD fits to RDLF data seen in Figure 5.

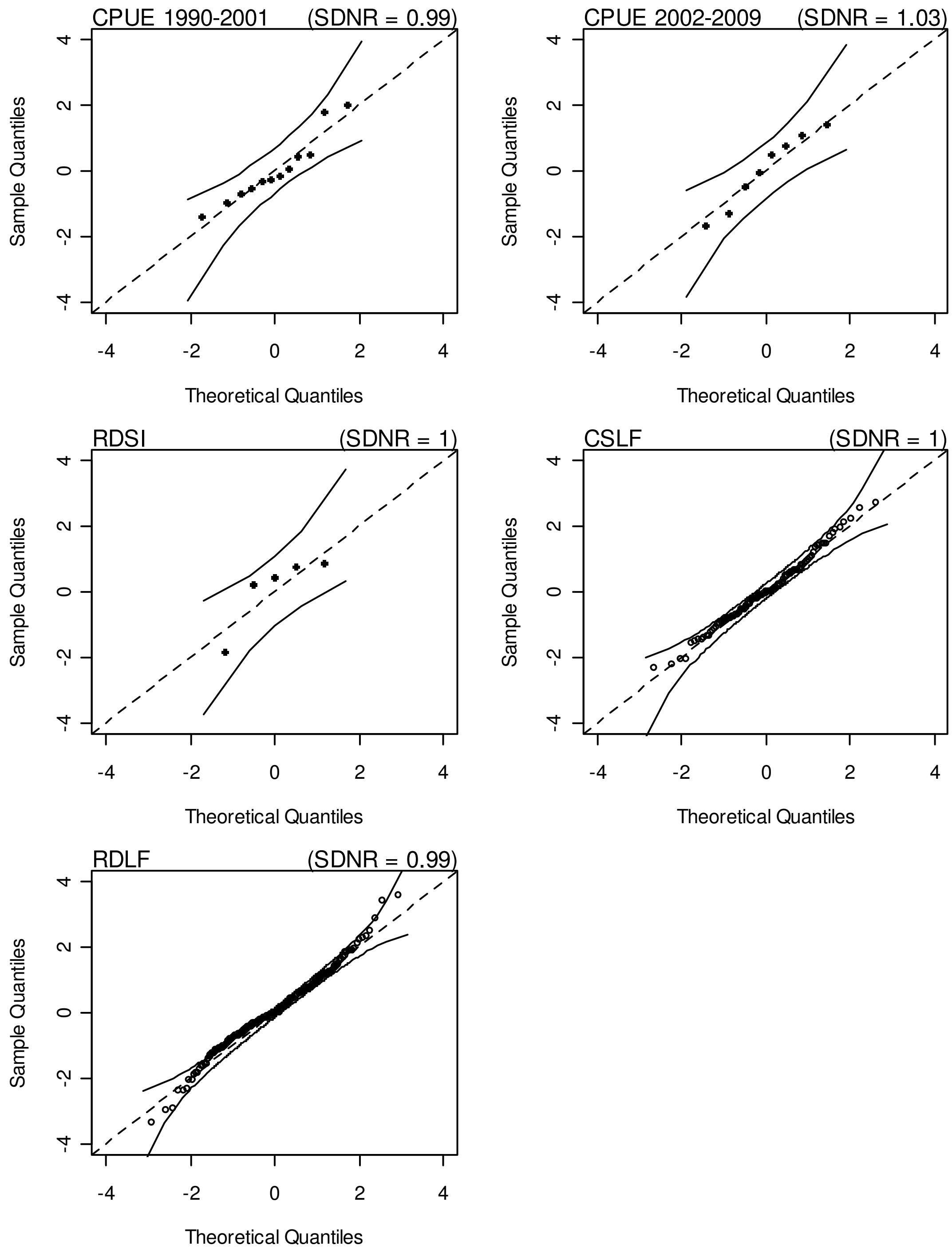

Figure 7: Q-Q plot of residuals for the fits to the CPUE, PCPUE, RDSI, CSLF, and RDLF from the initial model MPD fit.

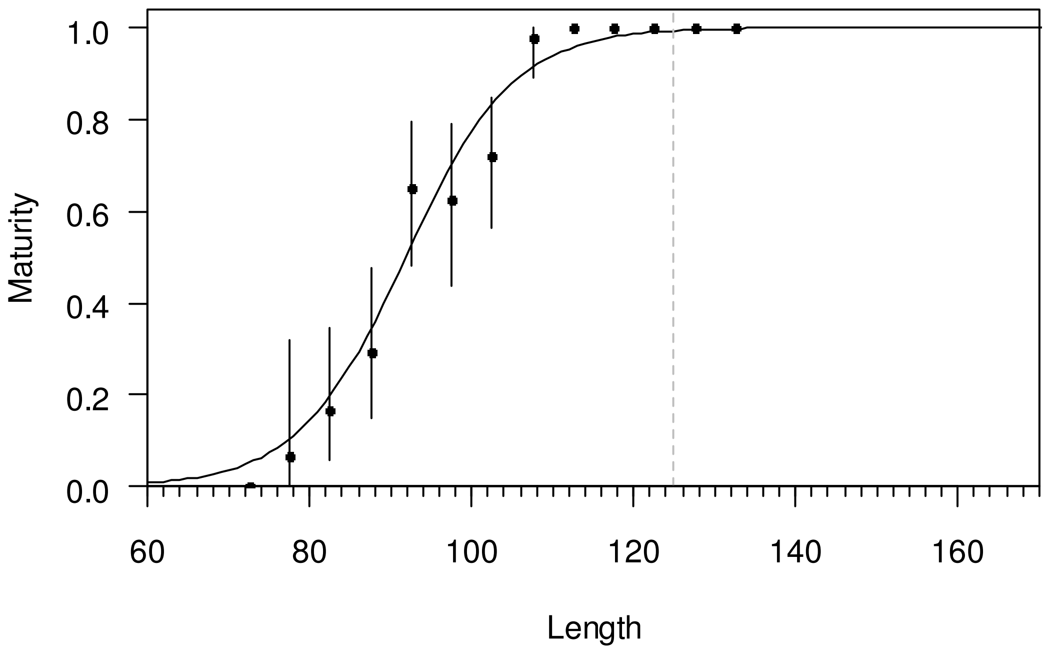

Figure 8: Observed (dots and vertical bars) and predicted proportion of maturity at length for the base case MPD fit. Vertical bars represent 95% interval of estimated proportion mature at each length bin. Dashed line represents the legal size limit of 125 mm.

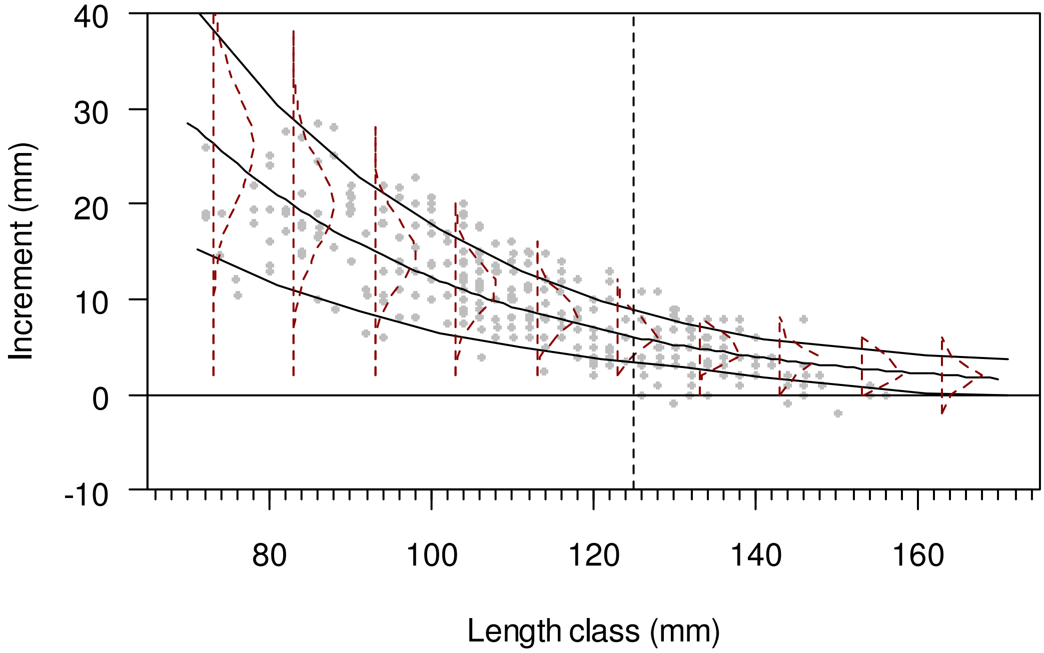

Figure 9: Observed mean annual increment at size from the growth data (dots), model estimated growth curve with 95% confidence interval (black lines), and model estimated growth transition matrix at selected sizes (dashed lines) for the base case MPD fit. The dashed vertical line represents the legal size limit of 125 mm.

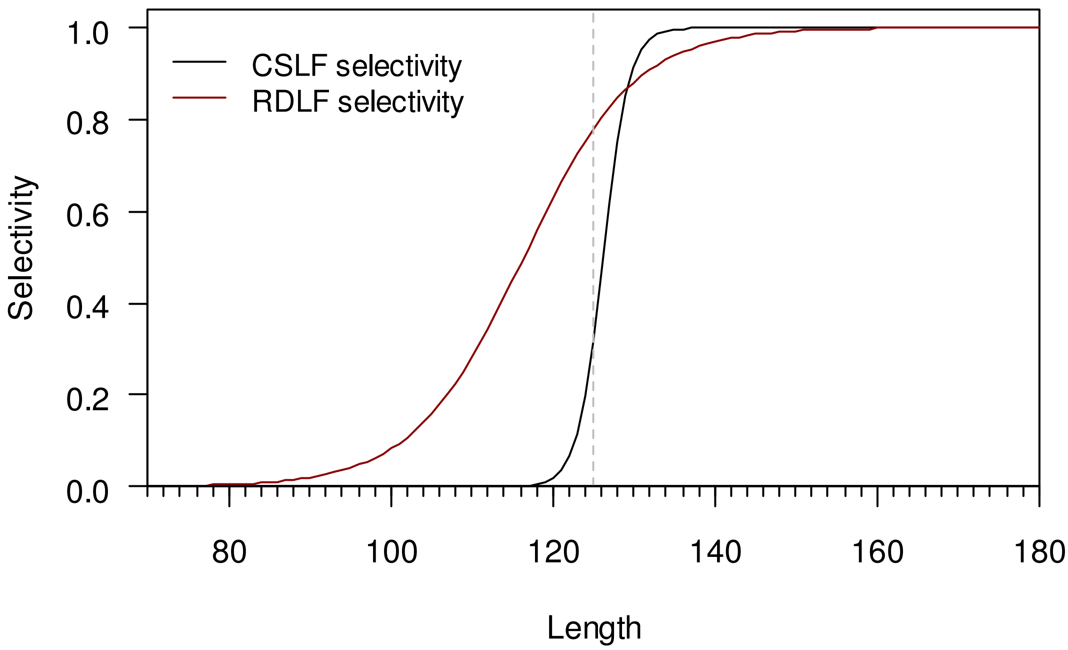

Figure 10: Estimated commercial and research diver selectivity from base case MPD fits. Dashed line represents the legal size limit of 125 mm.

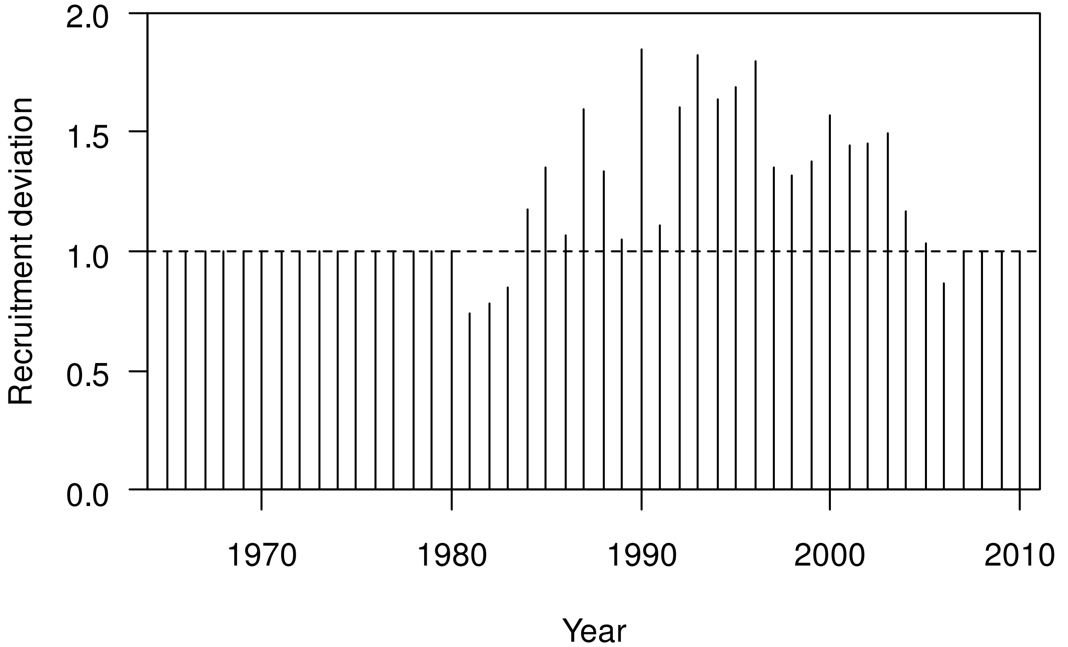

Figure 11: Recruitment deviations from base case MPD fits. Recruitment deviations were estimated for 1986–2006, and assumed to be fixed at 1 for other years.

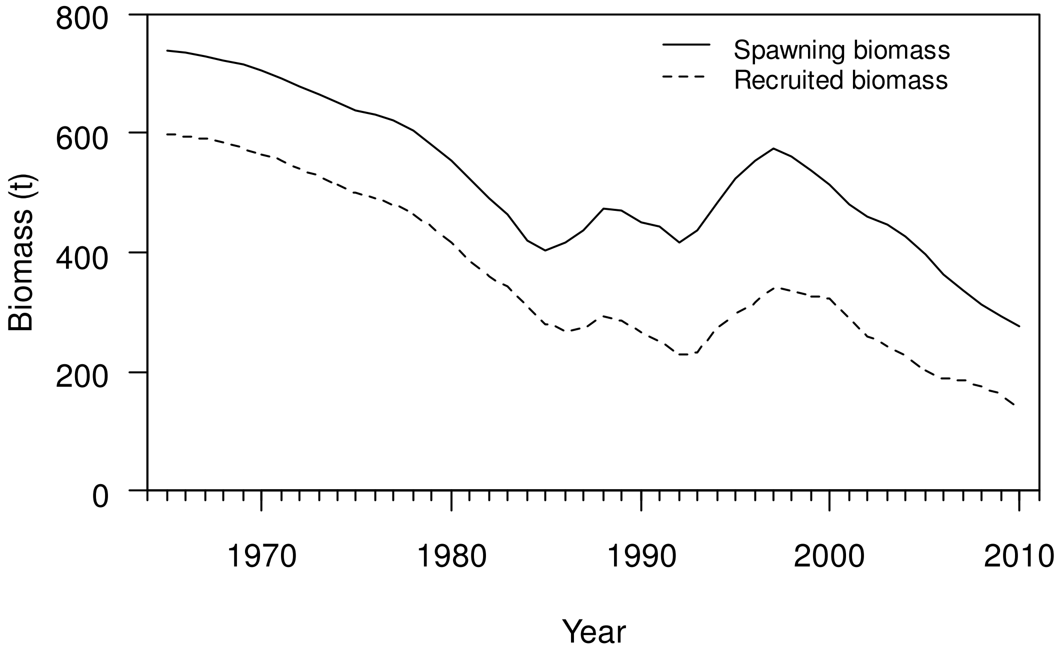

Figure 12: Spawning and recruited biomass trajectory from the initial model MPD fit.

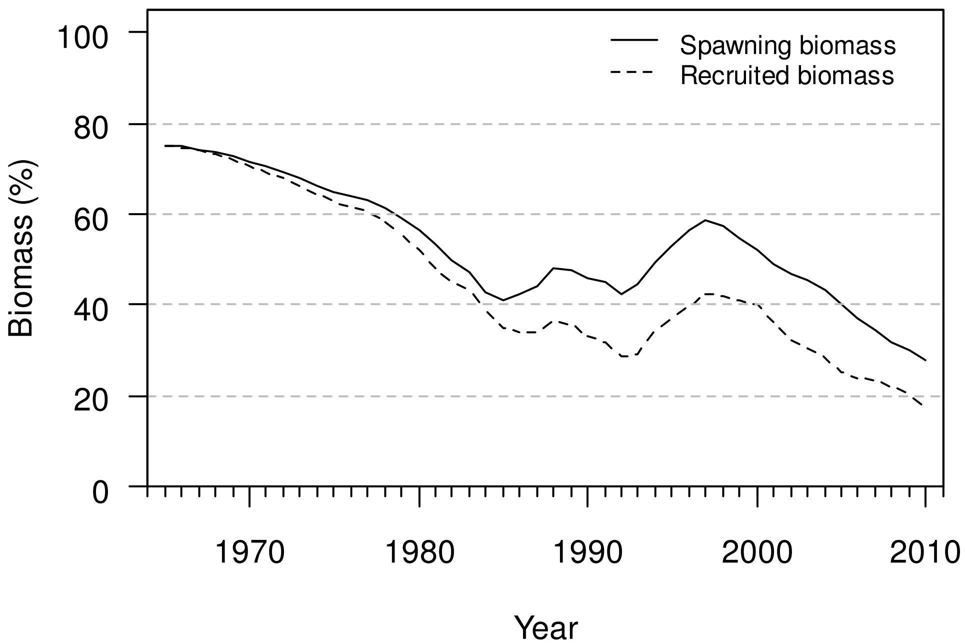

Figure 13: Spawning stock biomass as a percentage of B_0 and recruited biomass as a percentage of B_0^r from the initial model MPD fit.

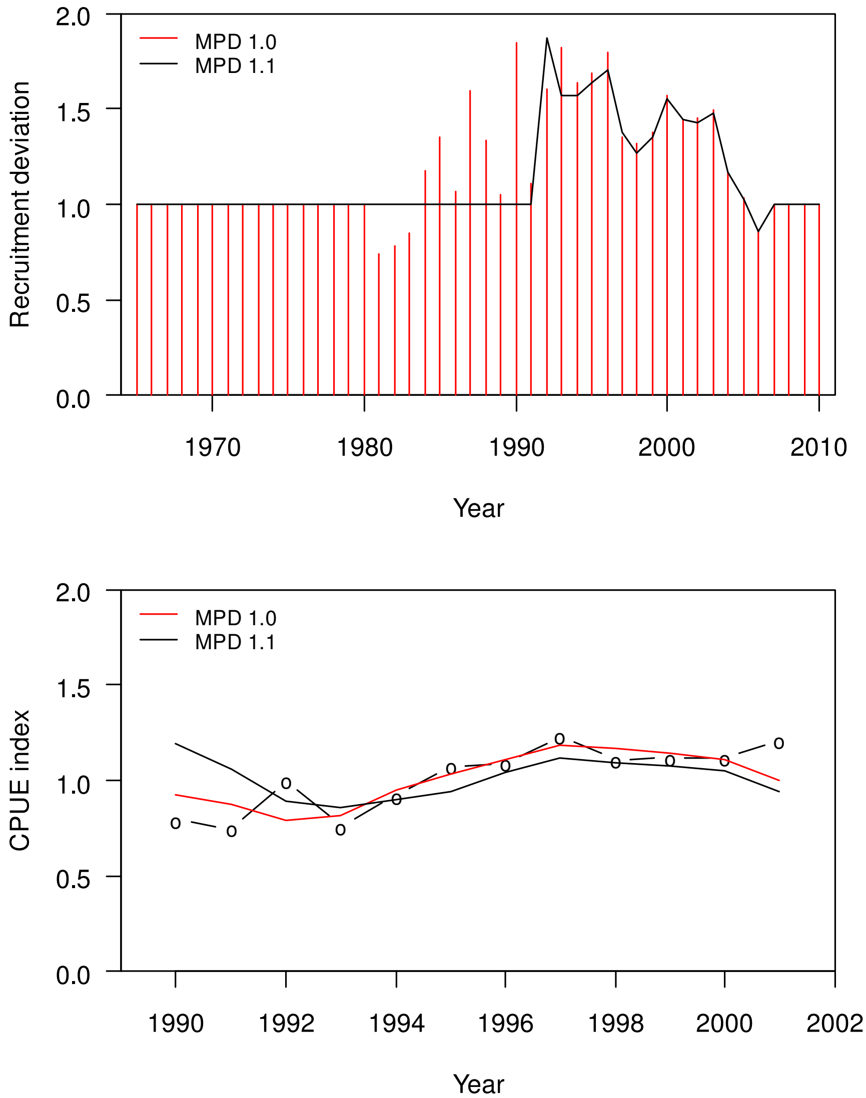

Figure 14: A comparison of MPD estimates of recruitment deviations (above) and fits to the early CPUE series 1990–2001 (below) between the model run 1.0 and 1.1.

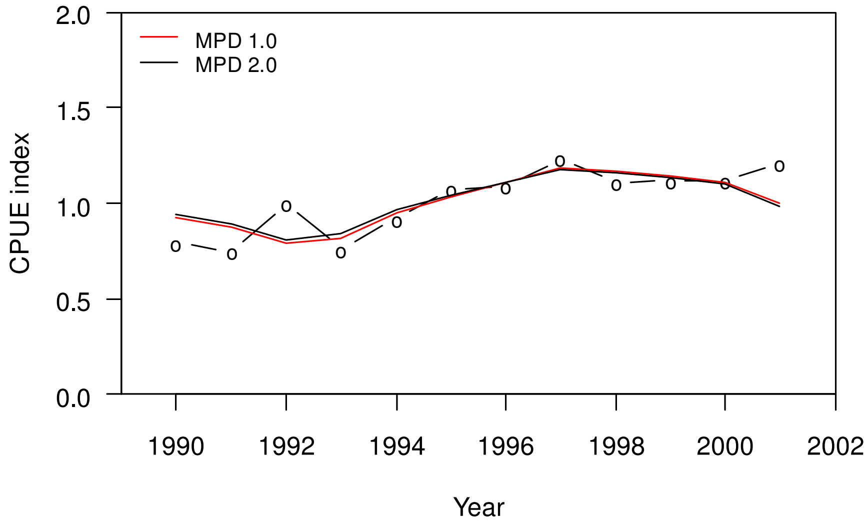

Figure 15: A comparison of MPD fits to the early CPUE series 1990–2001 between the model run 1.0 and 2.0.

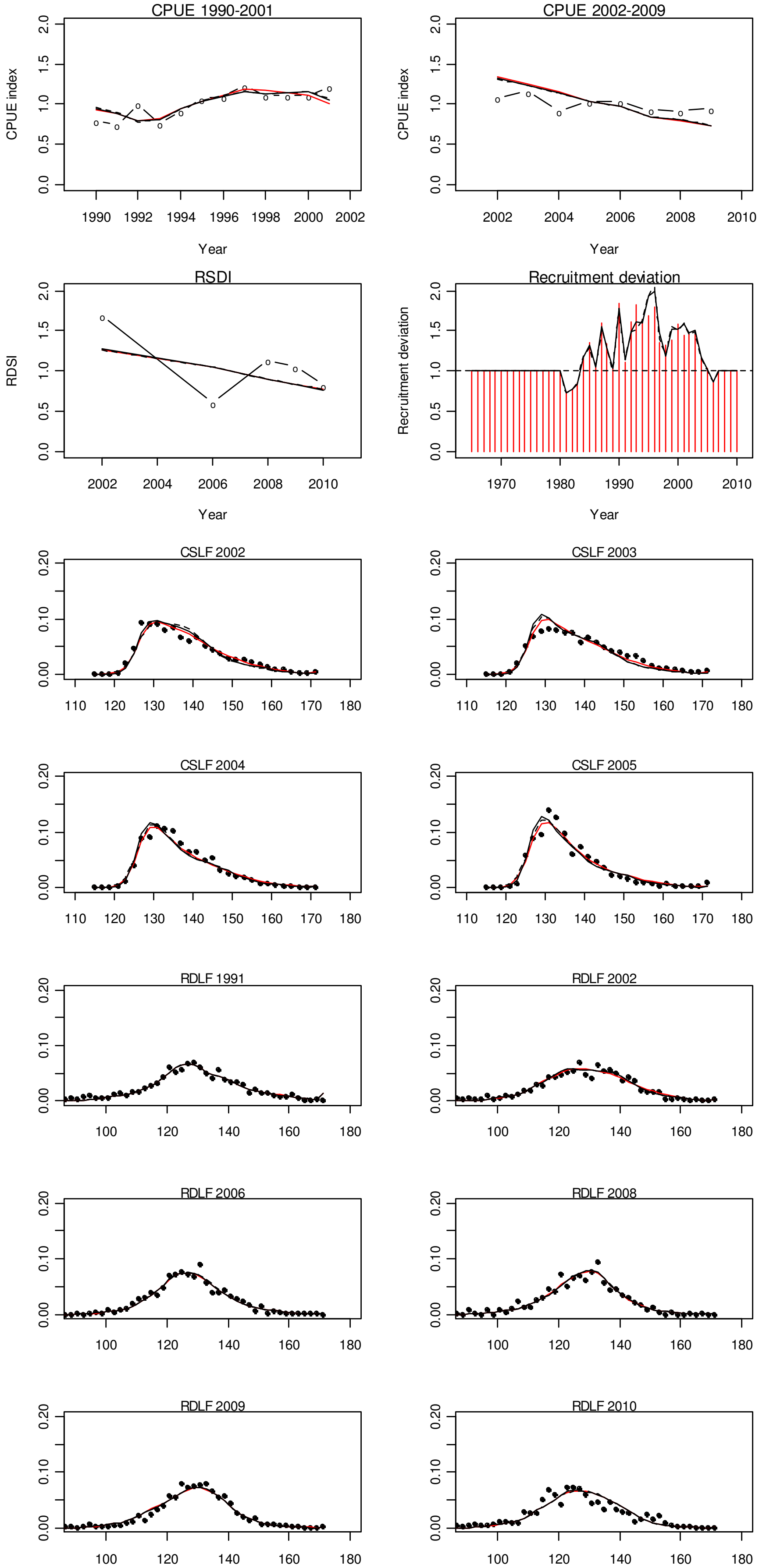

Figure 16: A comparison of MPD fits to the CPUE, RDSI, CSLF, and RDLF, and estimates of recruitment deviations between model run 1.0 (grey line), 3.0 (black solid line) and 3.1 (black dashed line). Observed values are shown in dots.

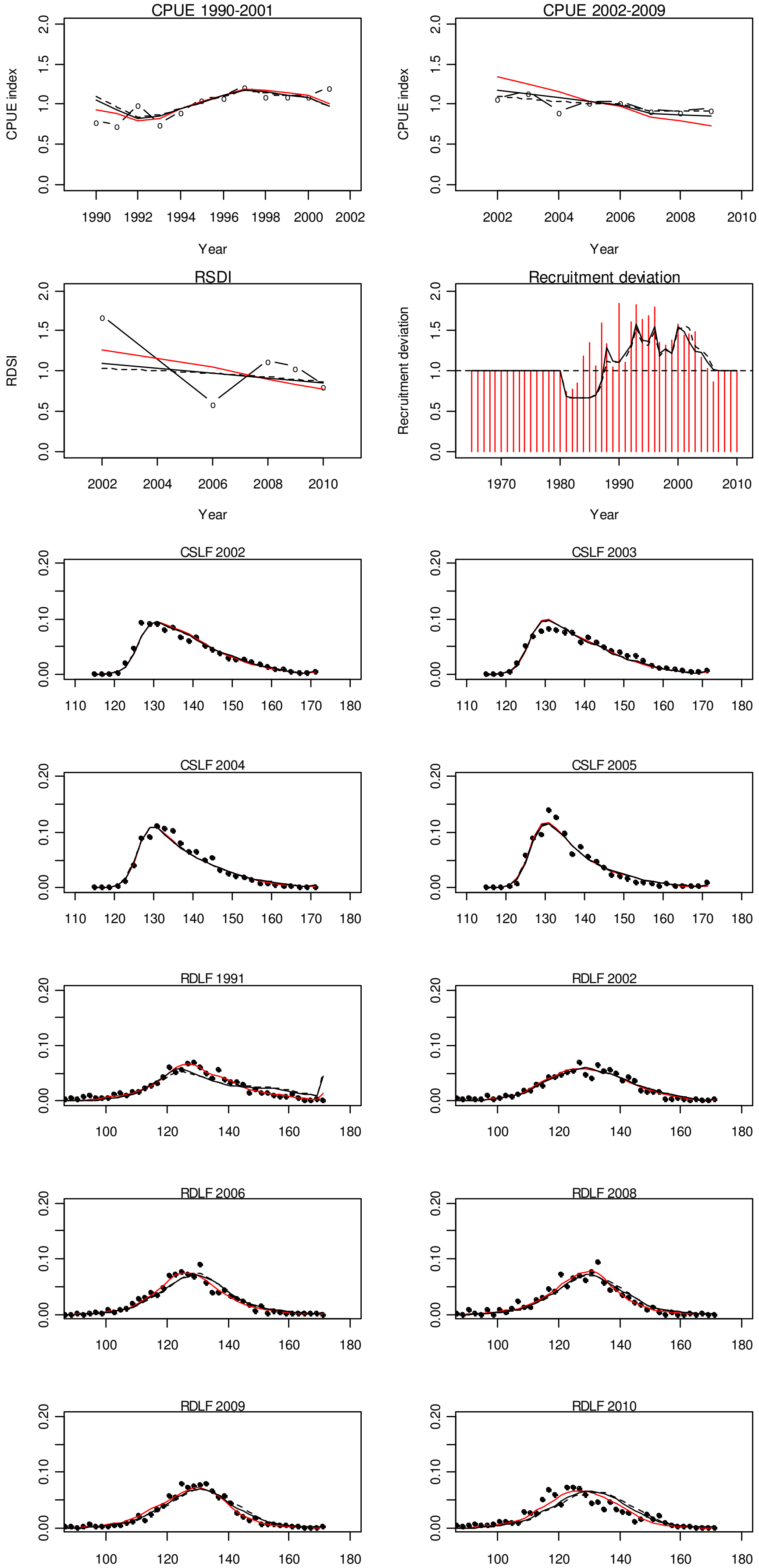

Figure 17 : A comparison of MPD fits to the CPUE, RDSI, CSLF, and RDLF, and estimates of recruitment deviations between model run 1.0 (grey line), 4.0 (black solid line) and 4.1 (black dashed line). Observed values are shown in dots.

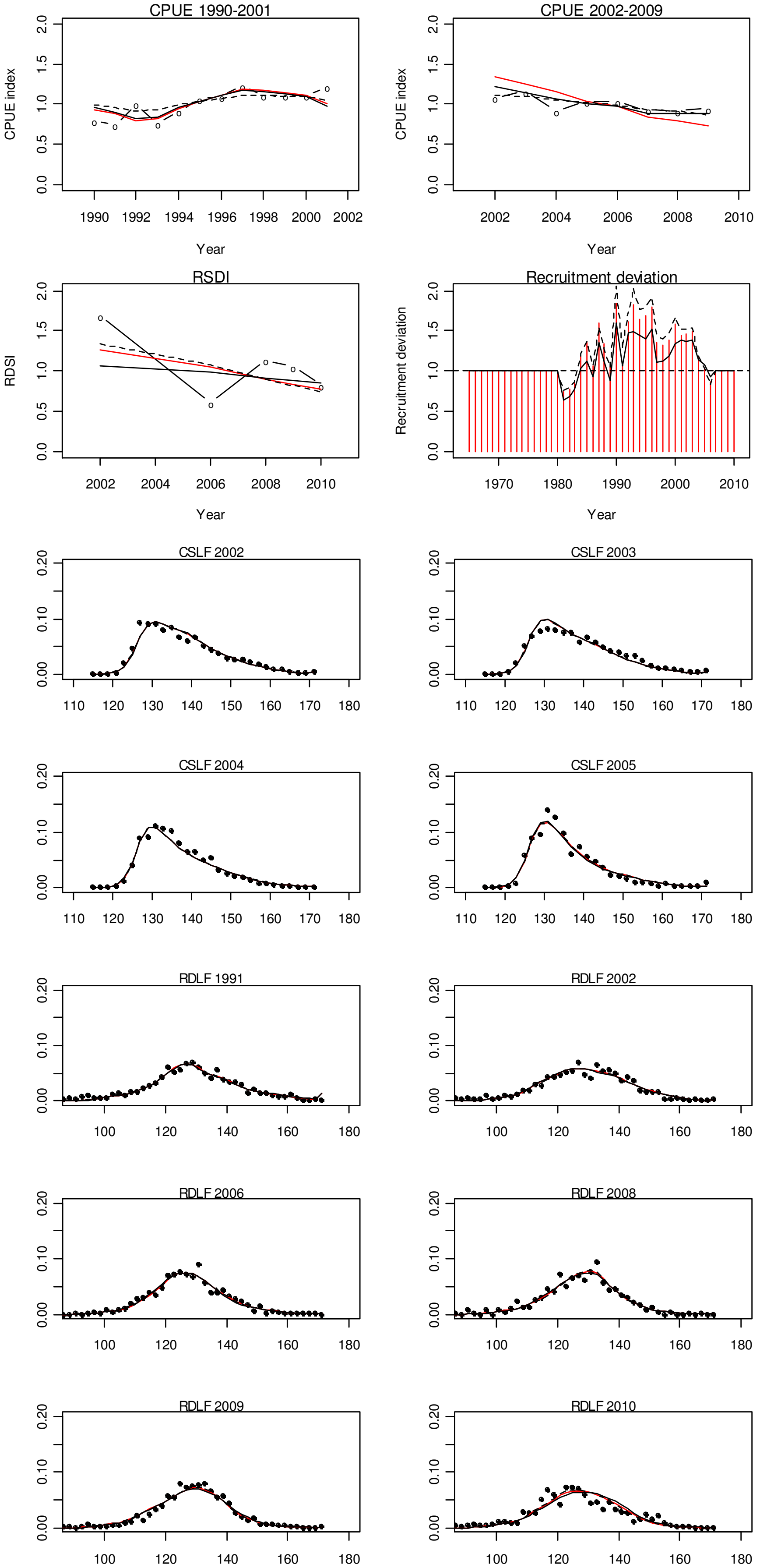

Figure 18 : A comparison of MPD fits to the CPUE, RDSI, CSLF, and RDLF, and estimates of recruitment deviations between model run 1.0 (grey line), 5.0 (black solid line) and 8.0 (black dashed line). Observed values are shown in dots.

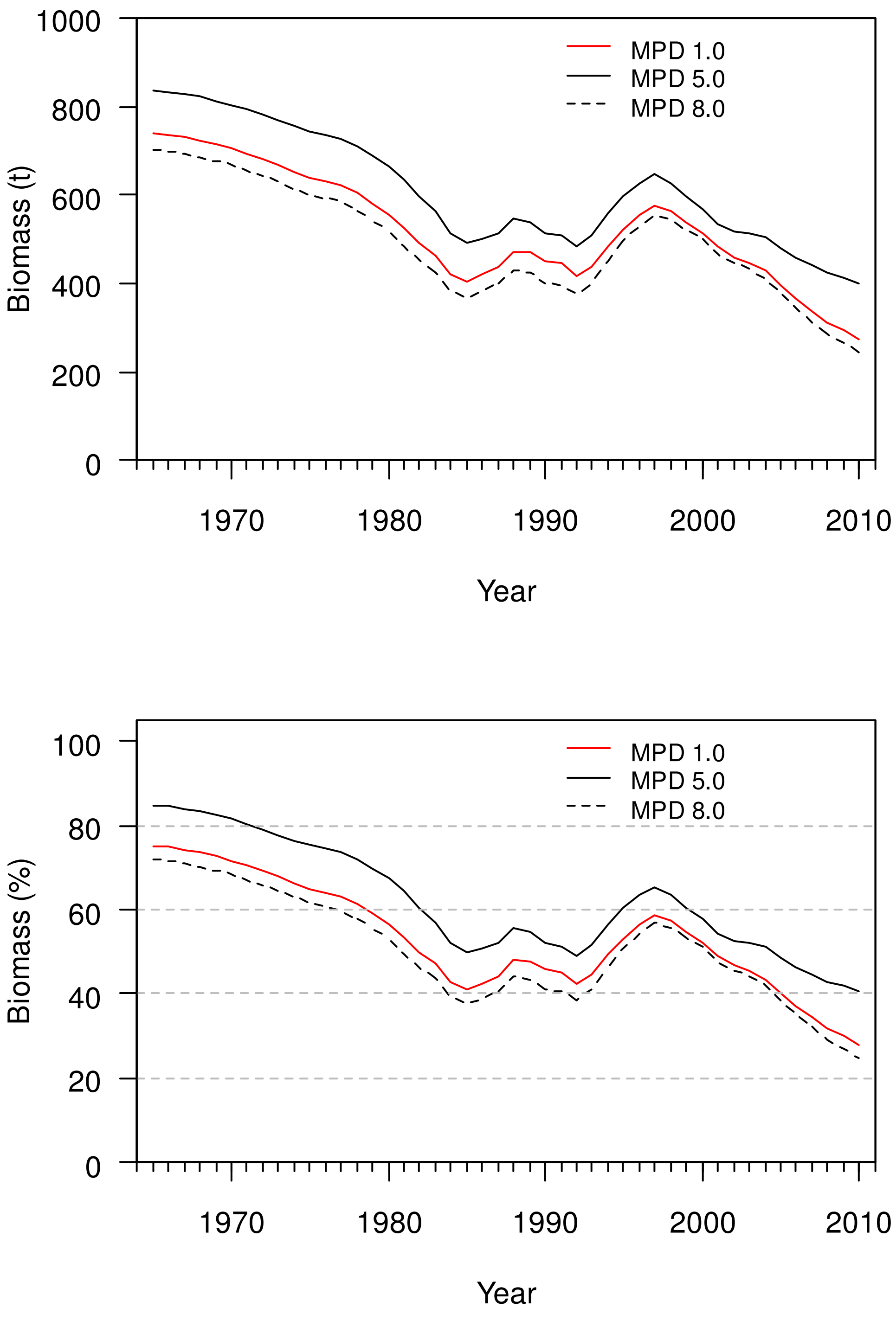

Figure 19 : A comparison of MPD estimates of the spawning biomass (top) and the spawning biomass as a percent of B_0 between model run 1.0 (red line), 5.0 (black solid line) and 8.0 (black dashed line).

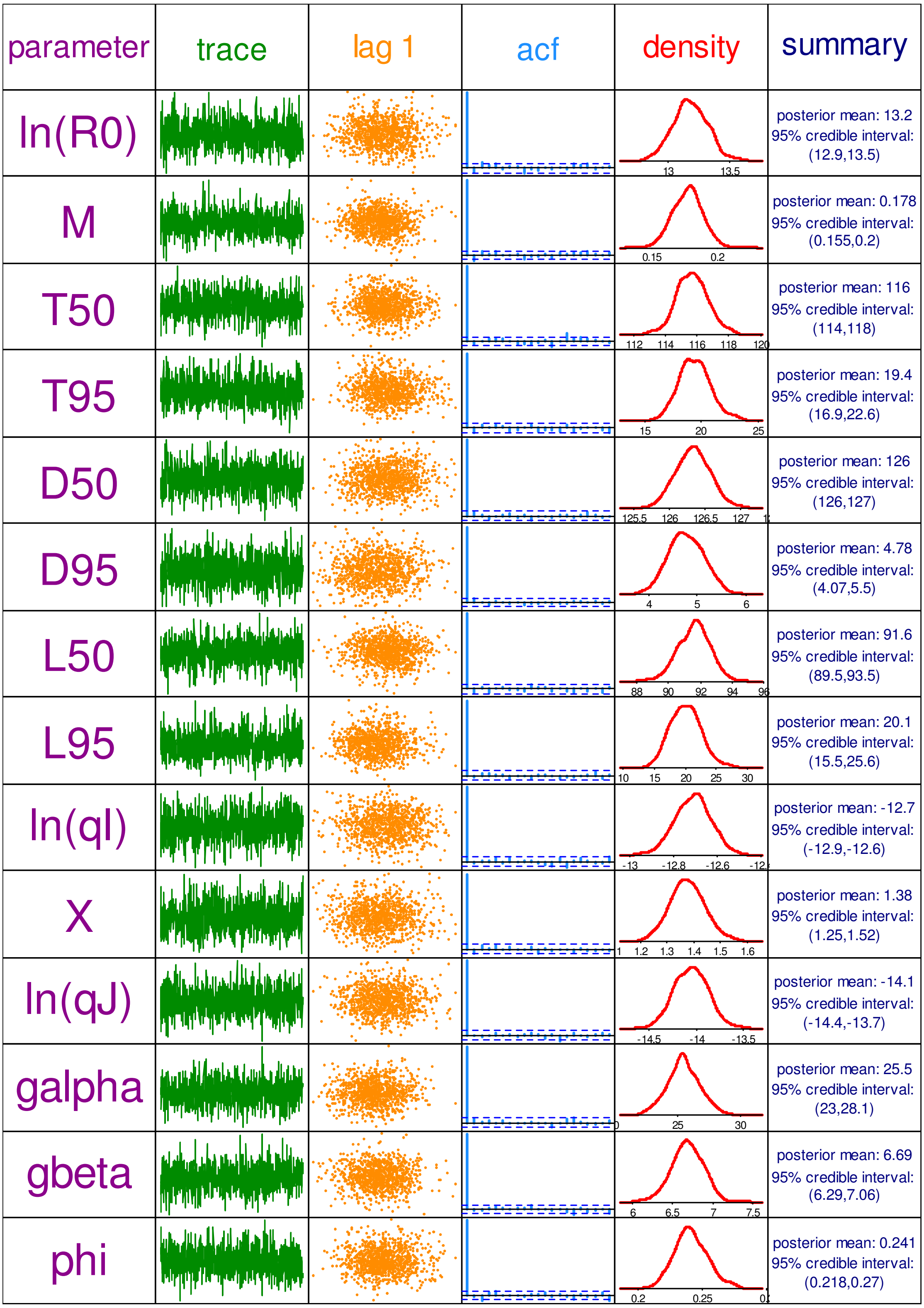

Figure 20: Diagnostics for the base case MCMC posterior samples of estimated parameters and indicators. "trace" is the trace plot of the sampled chain; "lag 1" is the i^{th} data plotted against the $i+1^{th}$ data in the chain; "acf" is the autocorrelation of the chain at lag 1, 2, …; "density" is the posterior distribution.

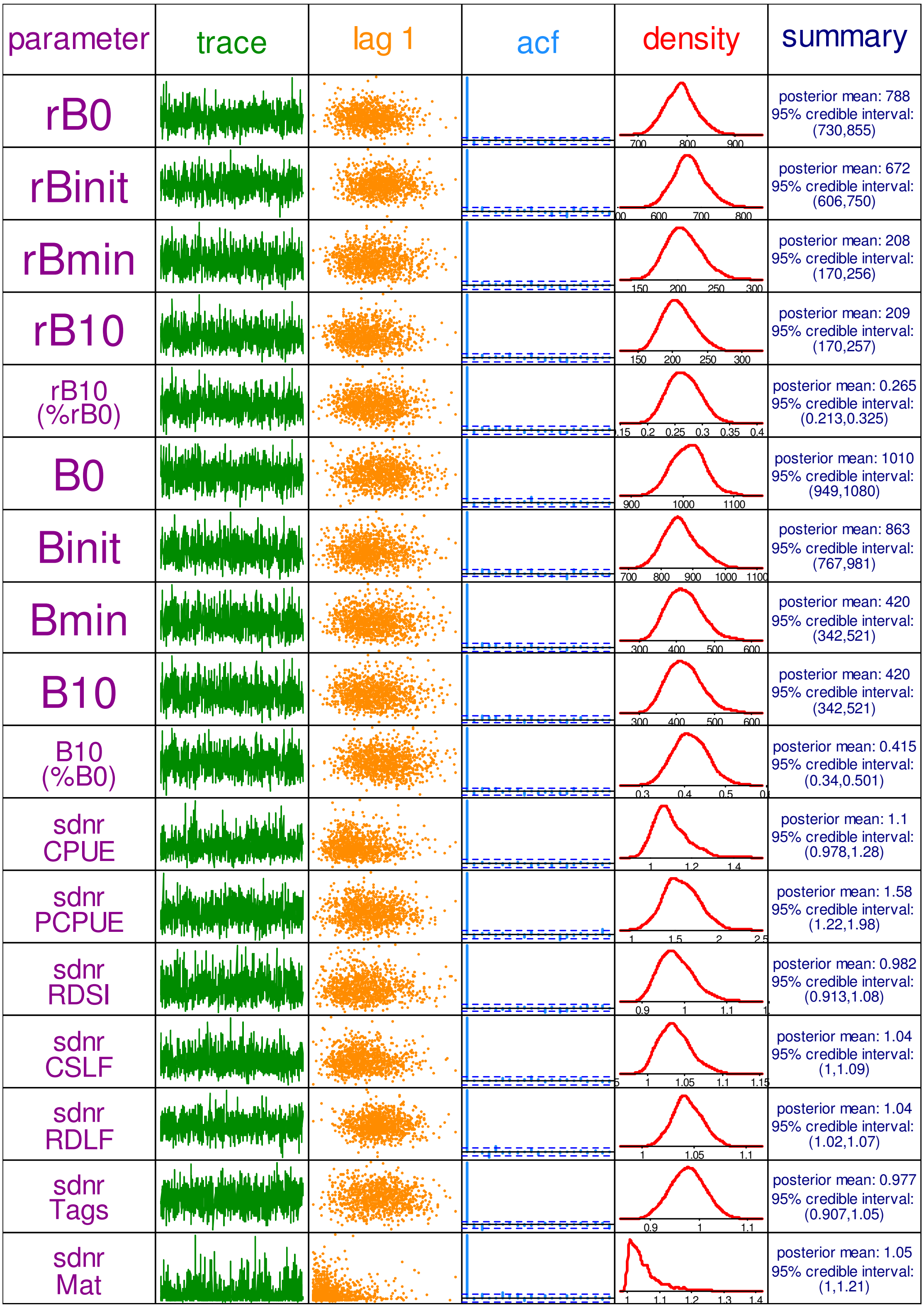

Figure 20–continued.

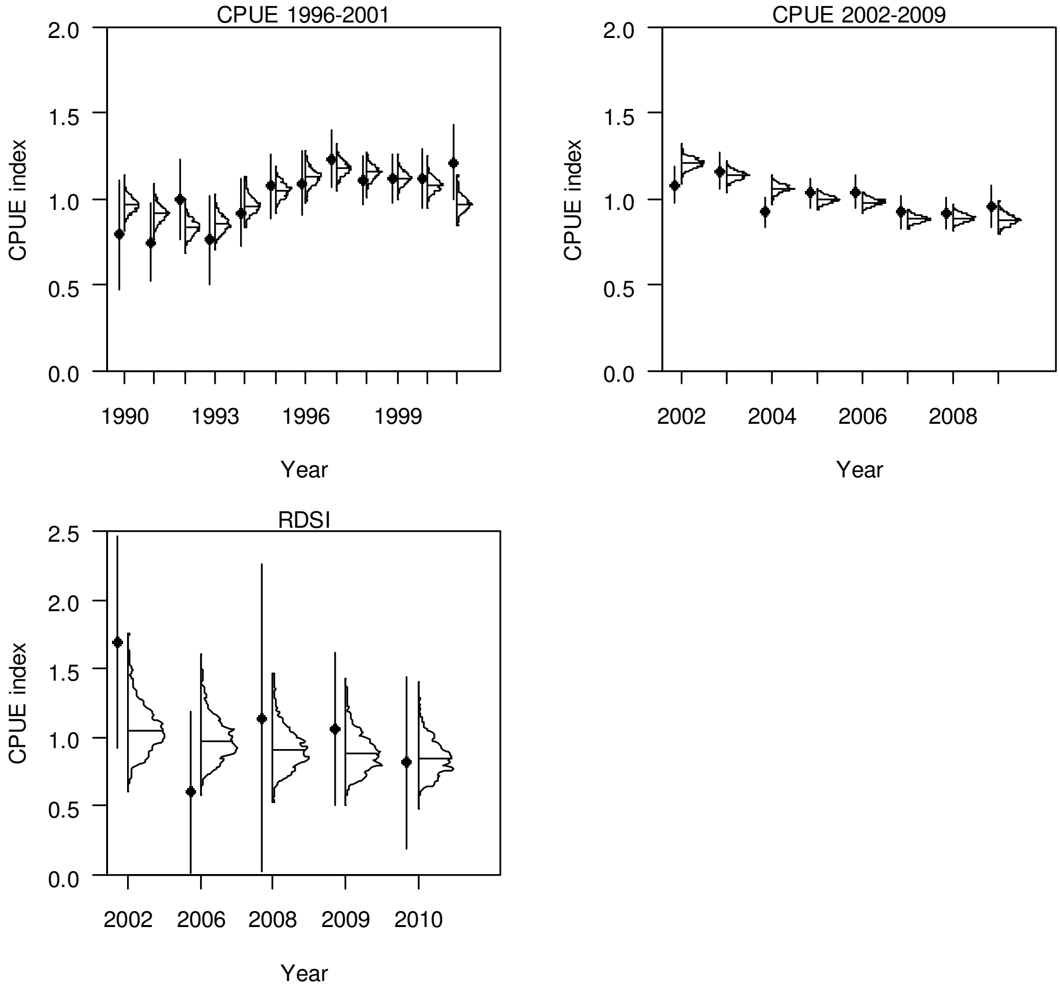

Figure 21: The posterior distributions of the fits to the early CPUE and recent CPUE, and the RDSI data for the base case MCMC. The dots are the observed data. Error bars show the standard error term used by the MPD model in fitting, including the effects of the common error term and the dataset weights.

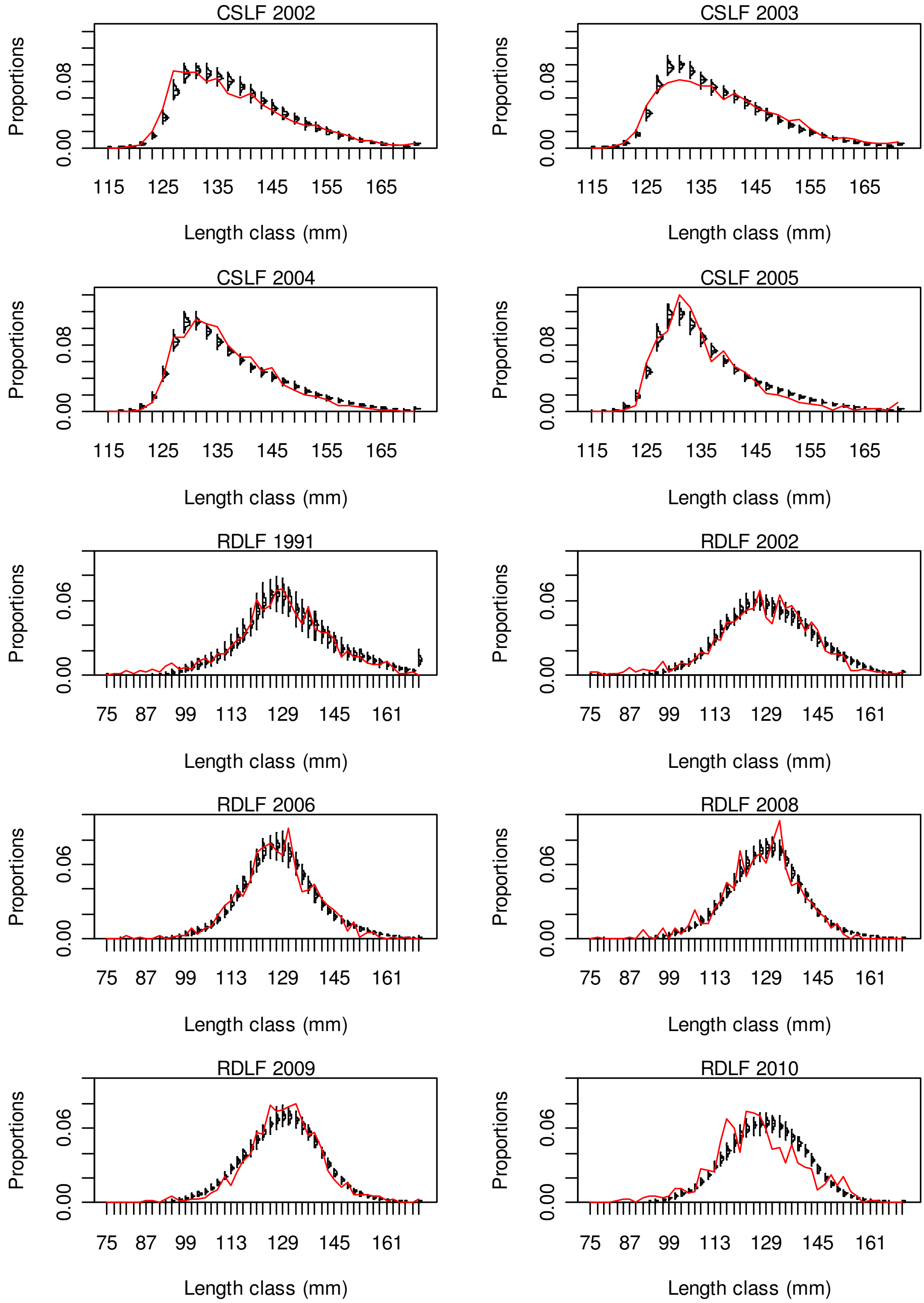

Figure 22: The posterior distributions of the fits to the CSLF and RDLF data for the base case MCMC. Lines are the observed data.

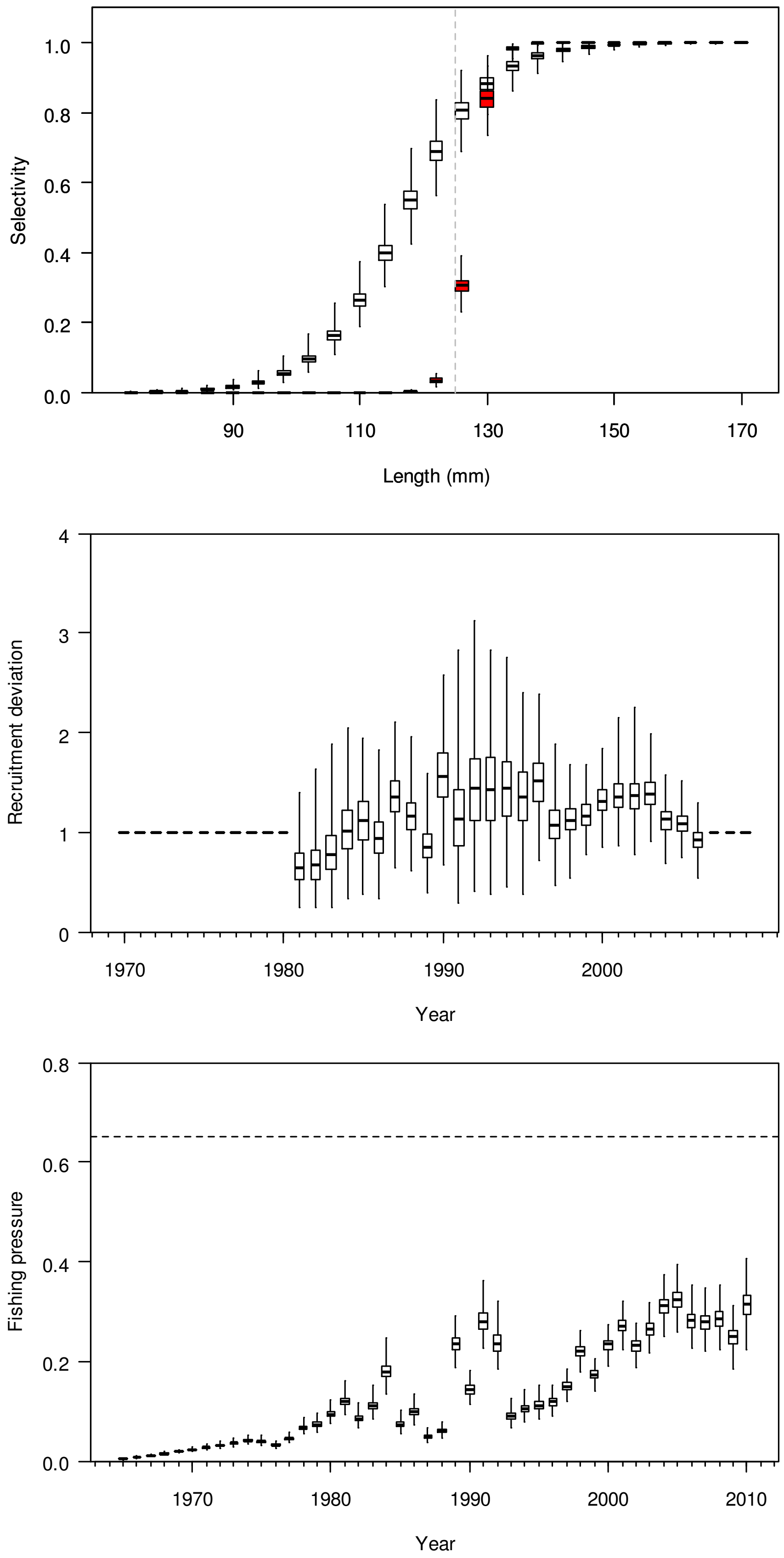

Figure 23: Posterior distributions of estimated commercial (grey) and research diver selectivity (top), recruitment deviations (middle), and exploitation rates (bottom) for the base case MCMC. The box shows the median of the posterior distribution (horizontal bar), the 25th and 75th percentiles (box), with the whiskers representing the full range of the distribution. Recruitment deviations were estimated for 1982–2006, and fixed at 1 for other years.

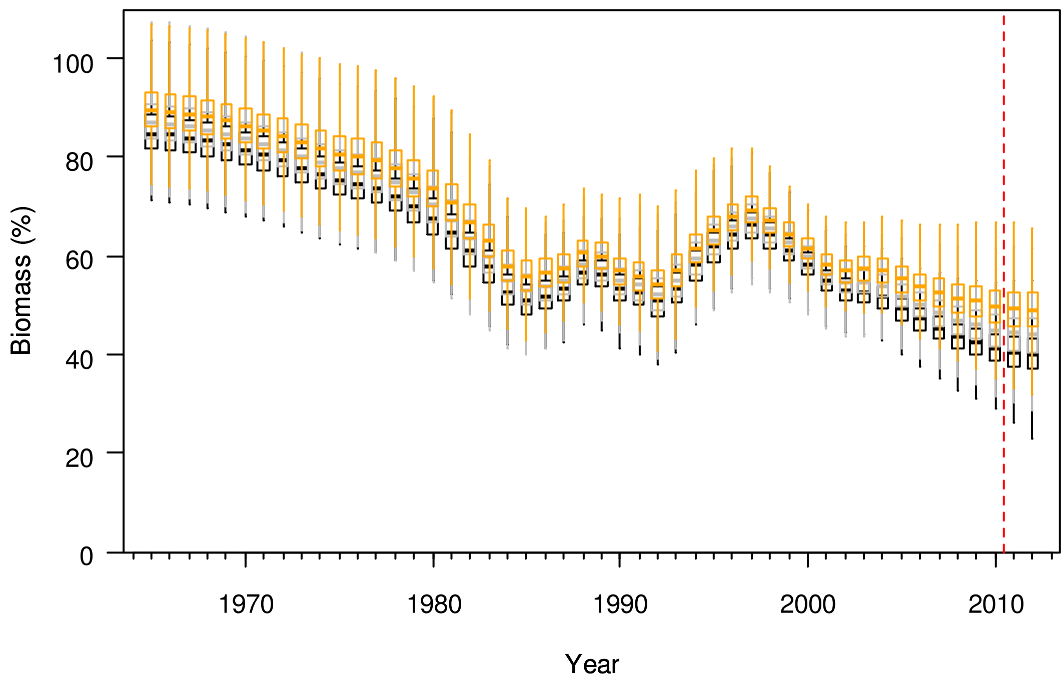

Figure 24: Posterior distributions of spawning stock biomass trajectory for model 5.0 (base case), 6.1, and 6.2. The box shows the median of the posterior distribution (horizontal bar), the 25th and 75th percentiles (box), with the whiskers representing the full range of the distribution. The boxes to the right of the dashed line indicate the projected spawning biomass to 2012 for each model assuming current catch level.

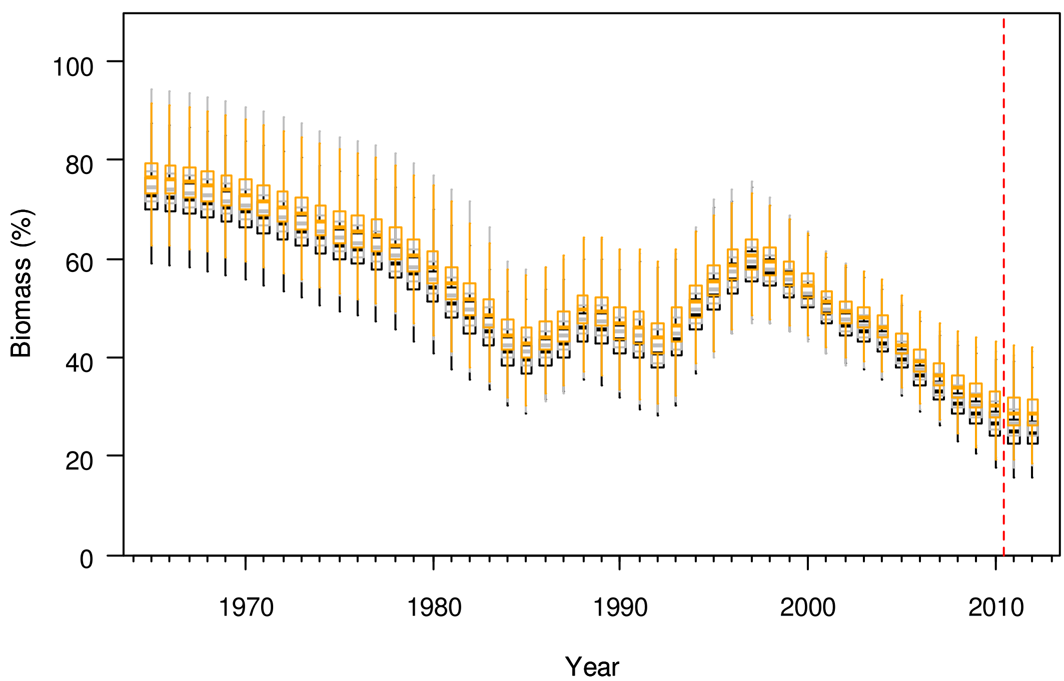

Figure 25: Posterior distributions of spawning stock biomass trajectory for model 8.0, 8.1, and 8.2. The box shows the median of the posterior distribution (horizontal bar), the 25th and 75th percentiles (box), with the whiskers representing the full range of the distribution. The boxes to the right of the dashed line indicate the projected spawning biomass to 2012 for each model assuming current catch level.

APPENDIX A: SUMMARY MPD MODEL FITS

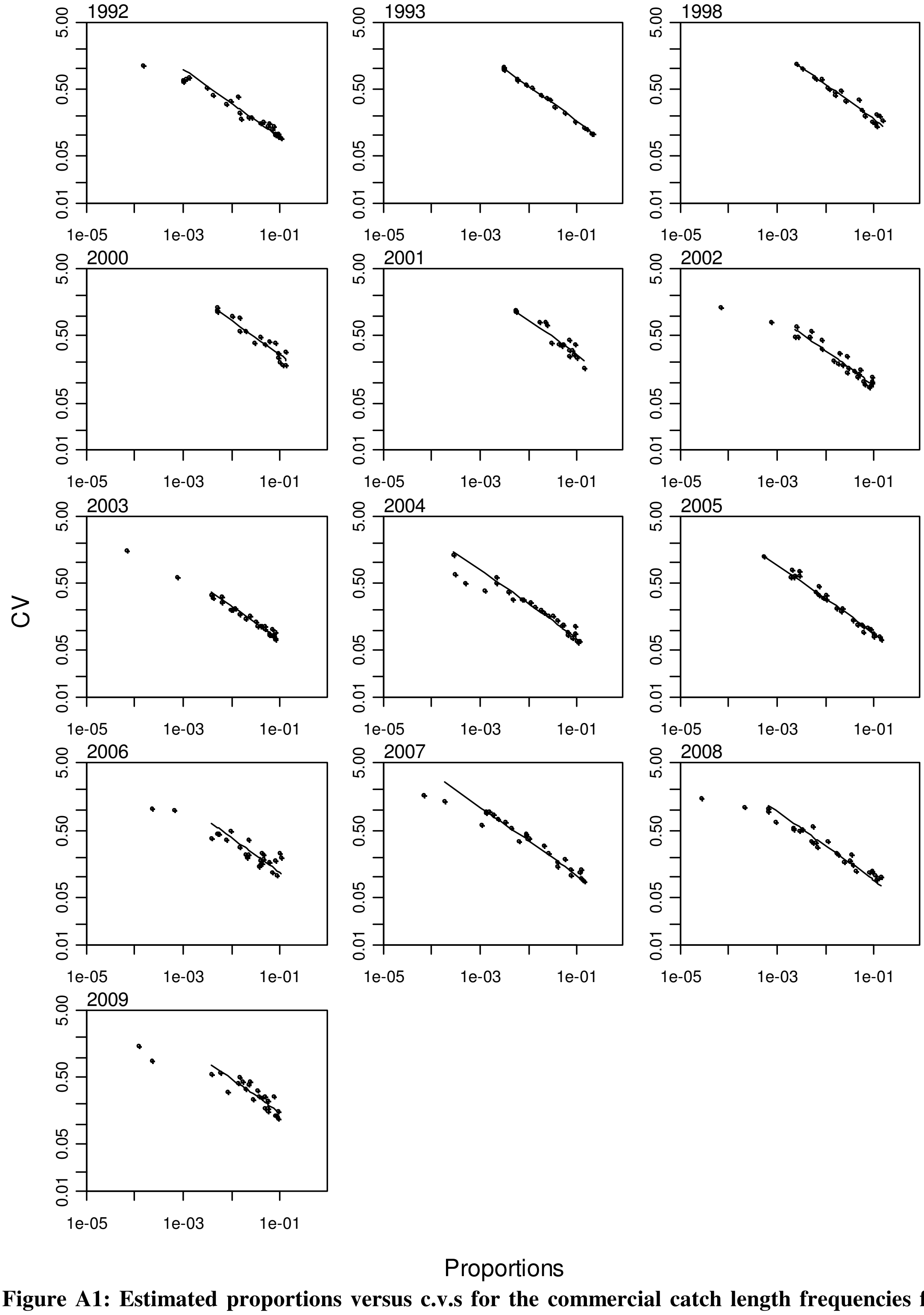

Figure A1: Estimated proportions versus c.v.s for the commercial catch length frequencies for Milford, George, Central, and Dusky combined for 1992, 93, 98, 2000–09. Lines indicate the best least squares fit for the effective sample size of the multinomial distribution. Note only the 2002–05 observations were used in the assessment model.

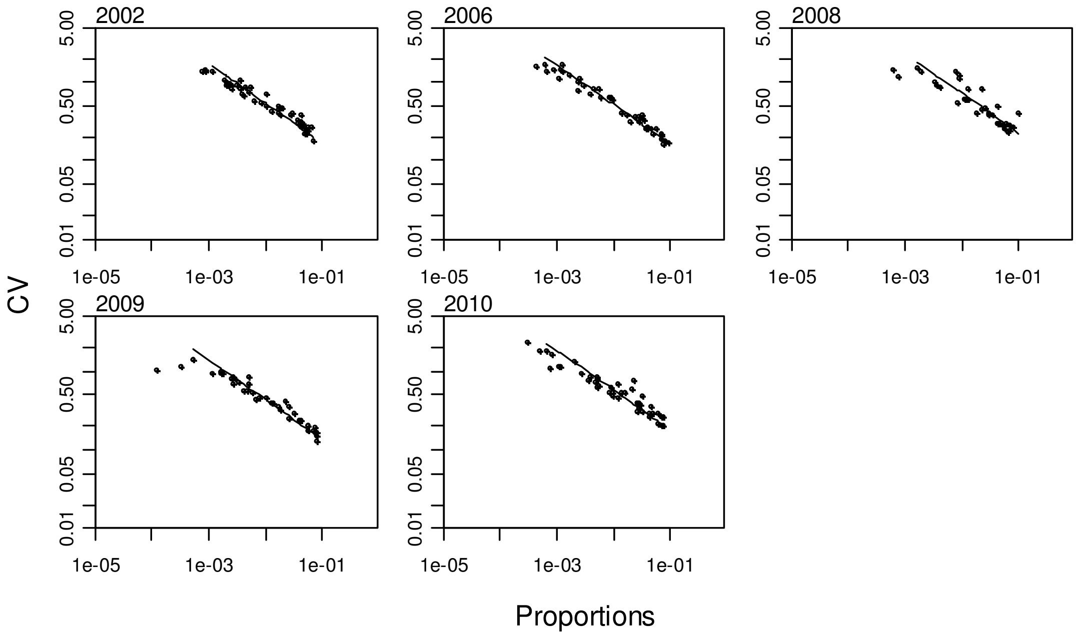

Figure A2: Estimated proportions versus c.v.s for the research diver length frequencies for Milford, George, Central, and Dusky combined for 2002, 2006, 2008–2010. Lines indicate the best least squares fit for the effective sample size of the multinomial distribution. C.V.S was not estimated for the 1991 sample as the unscaled length frequency was used.